US Army Corps of Engineers
Construction Engineering Research Laboratory

CERL Technical Report 99/37
May 1999

Robotic Underwater Corrosion Inspection/Assessment of Sheet Pile Along Two Rivers at Cleveland, Ohio

Cuyahoga River Bulkhead Study: Phase 2 Report

Charles P. Marsh
Robert Weber
James Klempir
Brian A. Temple

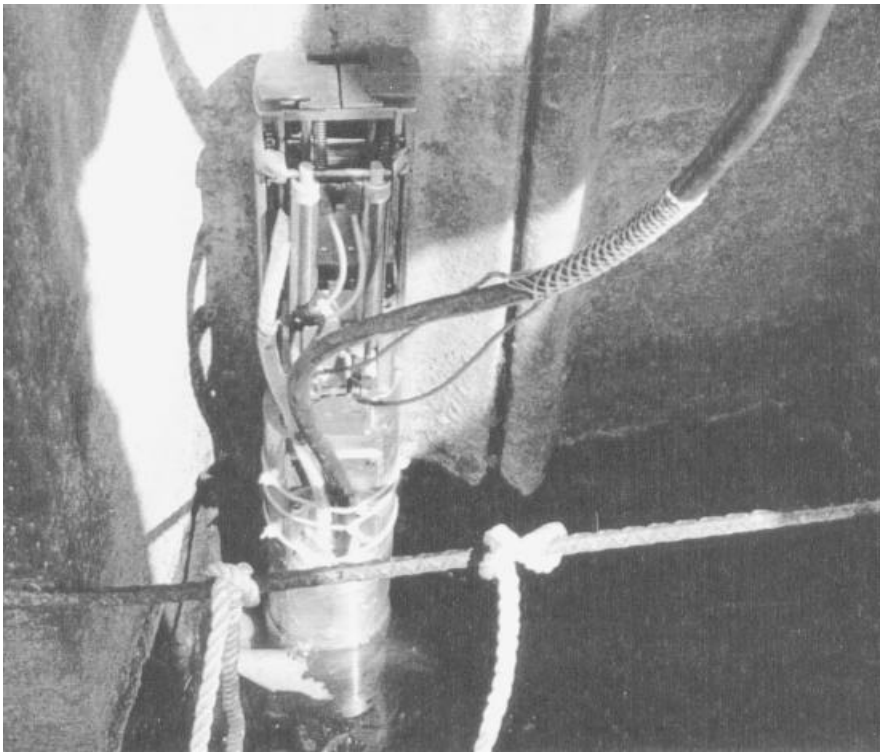

The objectives of this study were to (1) perform a quantitative underwater corrosion inspection and assessment of sheet pile along the Cuyahoga River at Cleveland and (2) use the measured material thicknesses and corrosion rates to predict a probable future range of sheet pile thickness. The work was conducted in response to The Water Resources Development Act of 1996, Section 438, which directs the Army to project the cost of repairing and/or replacing all sheet pile along the Cuyahoga River.

This Phase 2 work was a follow-on condition assessment, conducted by the U.S. Army Construction Engineering Research Laboratory (CERL), using a remotely controlled submersible robotic inspection system in conjunction with conventional hand-held acoustic thickness probes. Data were collected from 12 sites over a period of 1 week. Based on the data sample collected during the limited time frame of the study, a bounded, steady-state projection of future sheet pile condition was made for each site. Because corrosion rates correlate directly to the degree of zebra mussel infestation, these condition projections may be too conservative if zebra mussel infestation proceeds significantly faster than assumed in this study.

Foreword

This investigation was conducted for U.S. Army Engineer District Buffalo under Military Interdepartmental Purchase Request (MIPR) W81EU681485194, "Cuyahoga Bulkheads Inspection," dated 12 June 1998. The technical monitor was Teofilo D. Valerio, CELRD-PE-EE.

The work was performed by the Materials and Structures Branch (CF-M) of the Facilities Division (CF), U.S. Army Construction Engineering Research Laboratory (CERL). The CERL Principal Investigator was Dr. Charles P. Marsh. Robert Weber was the Associate Investigator, and James Klempir and Brian A. Temple were student contractors for the project. Dr. Ilker R. Adiguzel is Chief, CECER-CF-M, and L. Michael Golish is Chief, CECER-CF. The technical editor was Gordon L. Cohen, Information Technology Laboratory – CERL.

The Director of CERL is Dr. Michael J. O'Connor.

Contents

Foreword **2**

1 Introduction **7**

Background 7
Objectives 8
Approach 8
Mode of Technology Transfer 8
Units of Weight and Measure 9

2 Degradation Mechanisms of Sheet Pile **13**

3 Sheet Pile Thickness Measurements **15**

4 Corrosion Rate Measurements **19**

5 Video Inspection of Sheet Pile **23**

6 Discussion **27**

7 Summary and Recommendations **36**

Summary 36
Recommendations 36

References **37**

Figures **38**

Appendix A: Sites Referenced in Sheet Pile Thickness and Corrosion Rate Measurements **45**

Appendix B: Sheet Pile Thickness Measurements **71**

Appendix C: Sheet Pile Corrosion Rate Measurements **83**

Appendix D: Resistivity and Water Chemistry Data **92**

Distribution

List of Figures and Tables

Figures

Figure 1. Map of test site locations. 11
Figure 2. General principle of corrosion. 14
Figure 3. The Fury robot. 17
Figure 4. Use of the hand-held acoustic sensor. 18
Figure 5. McGyver measuring device. 18
Figure 6. Onsite probe for corrosion rate measurement. 19
Figure 7. Waterline video capture of sheet pile at Site 1. 23
Figure 8. Video capture of Site 1 at 10 ft below waterline. 25
Figure 9. Video capture of Site 1 at 25 ft below waterline. 25
Figure 10. Site 1 projected thickness over time. 29
Figure 11. Site 2 thickness projected over time. 30
Figure 12. Site 3 web thickness projected over time. 30
Figure 13. Site 4 flange thickness projected over time. 31
Figure 14. Site 5 web thickness projected over time. 31
Figure 15. Site 5 flange thickness projected over time. 32
Figure 16. Site 6 web thickness projected over time. 32
Figure 17. Site 7 web thickness projected over time. 33
Figure 18. Site 8 web thickness projected over time. 33
Figure 19. Site 9 flange thickness projected over time. 34
Figure 20. Site 10 flange thickness projected over time. 34
Figure 21. Site 11 flange thickness projected over time. 35
Figure 22. Site 12 web thickness projected over time. 35
Figure 23. Site 1 thickness measurements. 39
Figure 24. Site 2 thickness measurements. 39
Figure 25. Site 3 thickness measurements. 40
Figure 26. Site 4 thickness measurements. 40
Figure 27. Site 5 thickness measurements. 41
Figure 28. Site 6 thickness measurements. 41
Figure 29. Site 7 thickness measurements. 42

Figure 30. Site 8 thickness measurements..... 42
Figure 31. Site 9 thickness measurements..... 43
Figure 32. Site 10 thickness measurements..... 43
Figure 33. Site 11 thickness measurements..... 44
Figure 34. Site 12 thickness measurements..... 44
Figure 35: Corrosion process showing anodic and cathodic current 84
Figure 36. Coal storage at Site 4, the Mid-Continental Coke and Coal property. 89
Figure 37. Polarization resistance testing device. 89
Figure 38. Fury robot entering the water on the back flange of the sheet pile. 91
Figure 39. Fury nearly submerged, taking measurements on the front flange of sheet pile. 91

Tables

Table 1. Corrosion rate analysis data. 21
Table 2. Life-cycle projection table for the sheet pile. 28
Table 3. Estimated dates of construction by site. 29
Table 4. Site 1 thickness measurements. 71
Table 5. Site 2 thickness measurements. 72
Table 6. Site 3 thickness measurements. 73
Table 7. Site 4 thickness measurements. 74
Table 8. Site 5 thickness measurements. 75
Table 9. Site 6 thickness measurements. 76
Table 10. Site 7 thickness measurements. 77
Table 11. Site 8 thickness measurements. 78
Table 12. Site 9 thickness measurements. 79
Table 13. Site 10 thickness measurements. 80
Table 14. Site 11 thickness measurements. 81
Table 15. Site 12 thickness measurements. 82

1 Introduction

Background

The Cuyahoga and Old Rivers in Cleveland, OH, are important industrial and recreational waterways that provide access through Lake Erie to the Great Lakes and the St. Lawrence River. Along both banks of the Cuyahoga and Old Rivers is steel sheet pile bulkheads that were first installed in the 1940s and 1950s. The failure of any portion of this sheet pile would have serious economic and environmental impact, and would also present a public safety hazard. The responsibility for this sheet pile rests with the landowners, but a recent federal law — *The Water Resources Development Act of 1996* (Public Law 104-303, Section 438, "Cuyahoga River, Ohio" [12 October 1996]) — mandates that the Army develop estimates for the cost of repairing and/or replacing all sheet pile bulkhead along these waterfronts in Cleveland. To develop such estimates, the Army must first determine the current condition of this sheet pile.

A Phase 1 study of the subject infrastructure (URS Greiner, Inc. 1998) was conducted using the systematic, engineering-based visual condition assessment approach detailed in CERL Technical Report REMR-OM-9/ADA231916 (Greimann, Lowell, and James Stecker, *Maintenance and Repair of Steel Pile Structures*, December 1990). Phase 2 of the study was a follow-on condition assessment, conducted by the U.S. Army Construction Engineering Research Laboratory (CERL) and is documented in this report. In the Phase 2 study, underwater thickness measurements were made using a remotely controlled submersible robotic system called *Fury* (Marsh, Siddique, and Hock 1997). Additionally, corrosion rate measurements were taken at selected sites to provide a basis for predicting bulkhead conditions at any given time during the sheet pile life-cycle. Inherent in this inspection and assessment capability are the following advantages:

- more accurate cost estimation for repair or replacement
- better quantitative basis for prioritizing maintenance and repair (M&R) projects
- improved life-cycle utilization of the infrastructure
- improved ability to prevent or mitigate potential economic, environmental, and public safety hazards that may arise from sheet pile failure.

Objectives

The objectives of this study were to (1) perform a quantitative underwater corrosion inspection and assessment of sheet pile at specific sites selected by the sponsor of the work and (2) use the measured material thicknesses and corrosion rates to predict a probable future range of sheet pile thickness.

Approach

Twelve sites along the Cuyahoga and Old Rivers were selected for study (Figure 1) and prioritized by engineering personnel from Army Engineer District Buffalo, NY, with input from the Executive Director of the Flats Oxbow Association of Cleveland, an organization representing area riverfront businesses and property owners. These sites were specified in order to focus the study on stretches of sheet pile that appeared to range in condition from medium-good to medium-poor, which are the most difficult to accurately assess by visual inspection alone.

The Fury robotic system was used in the field at Cleveland for one work week to take underwater ultrasonic thickness measurements. Then, a corrosion engineer certified by the National Association of Corrosion Engineers (NACE) was employed to take localized corrosion rate measurements. By applying the localized corrosion rate to the current thickness measurements, the future material thickness at any future point in the sheet pile life cycle could be projected. To help further refine the corrosion life prediction, other critical measurements were also taken. These included soil-side resistivity measurements (where applicable and where access was obtainable), and water pH, dissolved oxygen, total dissolved solids, hardness, chlorides, sulfides, and sulfates.

Mode of Technology Transfer

The results of this study will be combined with the Phase 1 study (URS Greiner, Inc. 1998) by Buffalo District to meet the requirements of PL 104-303, Section 438.

Operational experience with Fury gained by CERL during this field study will be incorporated into future refinements of the system, enhancing the robot and condition inspection methodologies to promote adoption of this dual-use technology for additional Corps-specific applications.

Units of Weight and Measure

U.S. standard units of measure are used throughout this report. A table of conversion factors for Standard International (SI) units is provided below.

SI conversion factors		
1 in.	=	2.54 cm
1 ft	=	0.305 m
1 yd	=	0.9144 m
1 sq in.	=	6.452 cm^2
1 sq ft	=	0.093 m^2
1 sq yd	=	0.836 m^2
1 cu in.	=	16.39 cm^3
1 cu ft	=	0.028 m^3
1 cu yd	=	0.764 m^3
1 gal	=	3.78 L
1 lb	=	0.453 kg
1 kip	=	453 kg
1 psi	=	6.89 kPa
°F	=	(°C x 1.8) + 32

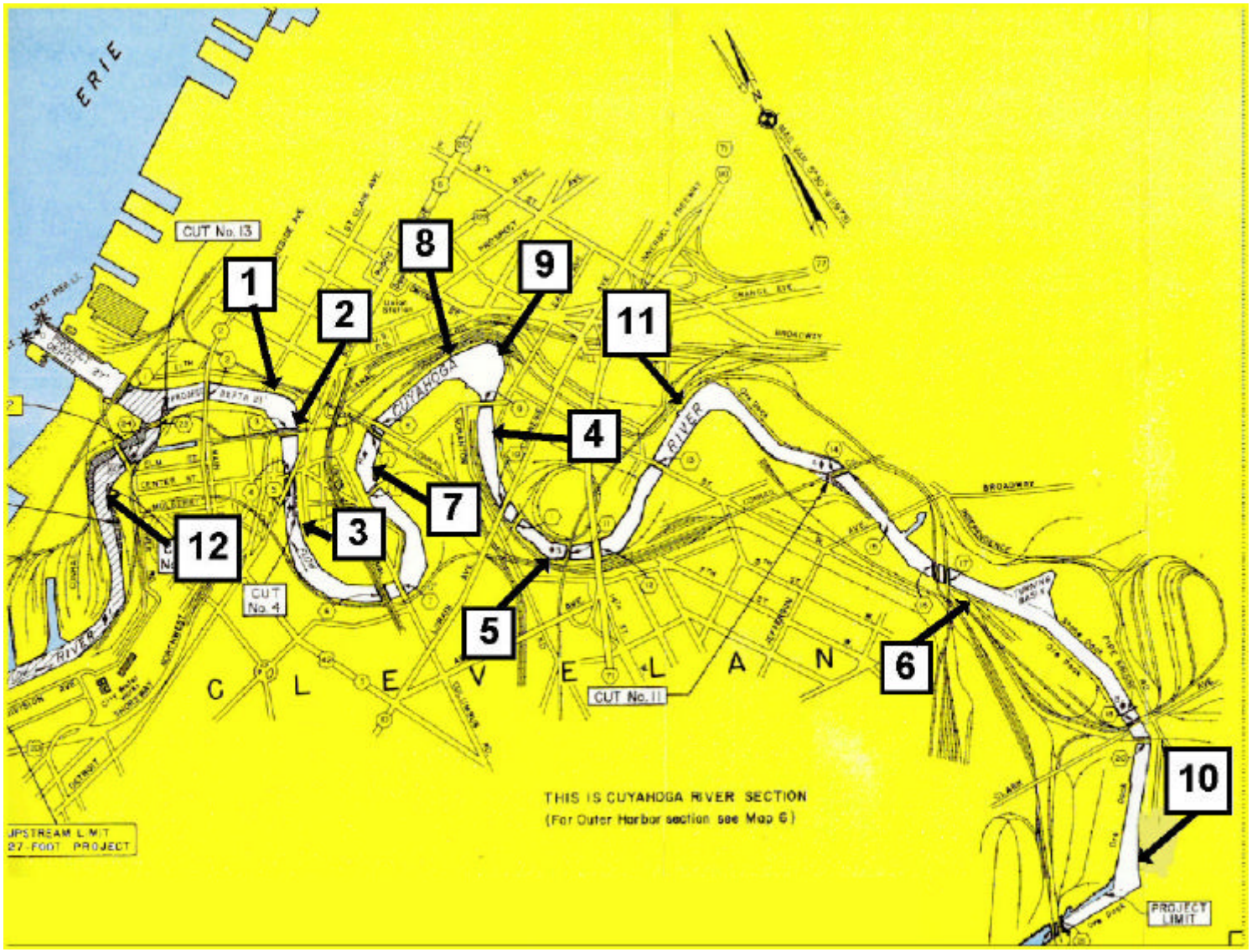

Figure 1. Map of test site locations.

2 Degradation Mechanisms of Sheet Pile

In an aqueous environment, the corrosion of steel is the result of a naturally occurring electrochemical process (Figure 2). If metal is in contact with such electrolytes as water or moist soil, variations in potential difference are formed due to factors such as local variations in retained stress from manufacturing, alloying elements and phase distribution, coating efficiency, and dissolved oxygen distribution. The potential difference creates small local cells that act like batteries. At anodic areas, dissolution of the metal occurs, producing ferrous ions and electrons as follows:

$$Fe \rightarrow Fe^{++} + 2e^{-}$$

On the other hand, at cathodic areas, electrons are consumed as shown below, depending on the electrolyte conditions:

$$2H^{+} + 2e^{-} \rightarrow H_2 \quad \text{and/or} \quad \frac{1}{2}O_2 + H_2O + 2e^{-} \rightarrow 2(OH)^{-}$$

While steel goes into solution at the anodes as ferrous ion, where there is sufficient oxygen available, this metal will be rapidly converted to insoluble hydrated ferric oxides that deposit on the surface as rust.

$$Fe^{++} + 2(OH)^{-} \rightarrow Fe(OH)_2$$

$$2Fe(OH)_2 + \frac{1}{2}O_2 + H_2O \rightarrow 2Fe(OH)_3$$

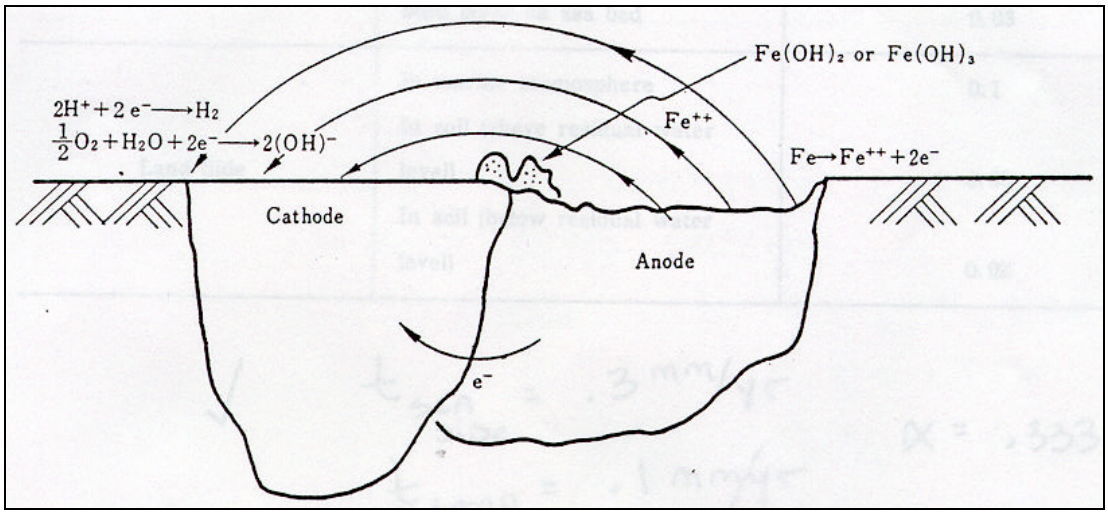

Figure 2. General principle of corrosion.

In the Cuyahoga and Old Rivers, the regular passage of river traffic serves to provide a sufficient supply of dissolved oxygen to allow the oxidation process to continue more or less uniformly as general corrosion. On the soil side of the sheet pile, soil resistivity determines how easily corrosion currents flow in the soil. The corrosion current is directly proportional to the amount of metal lost. The lower the resistance (i.e., soil resistivity), the greater the rate of corrosion and metal loss.

An additional factor affecting the degradation of the sheet pile is the presence of zebra mussels. The infestation at the time of this work appeared to be well advanced in Lake Erie,* but decreased the farther inland the designated site was located. Although the mechanism is not yet fully understood, recent experience with inland waterway infestation by zebra mussels indicates an accelerated corrosion rate compared to the corrosion rate without zebra mussels (Claudi and Mackie 1994; Race and Kelly 1996).

* As observed at the Corps of Engineers' Cleveland Area Office.

3 Sheet Pile Thickness Measurements

From 24 – 28 August 1998, the inspection team* conducted sheet pile thickness measurements. Twelve sites, detailed in Appendix A, were chosen by the Buffalo District as indicative of the condition of sheet pile along the Cuyahoga and Old Rivers. Thickness measurements were taken by three methods.

The Fury robot was the primary means of data acquisition. Originally designed for thickness measurements in underground storage tanks, adaptation of Fury for this application was novel and cost effective. Figure 3 shows the robot, which consists of permanent magnetic wheels, bump sensors, steering head, and cleaning head with ultrasonic transducers. Not shown, in addition, are a TestPro Infometric Data Processor for the thickness measurement transducer and a control console.

Hand-held acoustic sensors were the primary backup method for thickness measurements. A Panametrics 5 MHz ultrasonic transducer with an Epoch III Model 2300 Data Processor were used to make the measurements. The transducer is attached to a pole and the pole is used to hold the sensor against the sheet pile while measuring. Figure 4 shows the method of use for the hand held sensor.

An additional backup device nicknamed “McGyver” was used to take acoustic measurements. Difficulties maintaining adequate pressure at increasing depths with the hand-held device led to the use of the McGyver, which is a wooden platform with a spring-loaded transducer holder that attaches to the steel sheet pile using permanent magnets. The Panametrics transducer system was used with the McGyver platform. Figure 5 illustrates the implementation of McGyver for sheet pile measurements.

The acquired data from the 12 surveyed sites were entered into a spreadsheet and plotted. The results from each site are plotted on a graph. The location of

* Consisting of personnel from CERL (Dr. Charles Marsh, Mr. Robert Weber, Dr. Aaron Averbuch, Mr. Brian Temple) and Buffalo District (Mr. Dennis Rimer).

each site is given in Appendix A, the data tables are in Appendix B, and the plots are provided under “Figures” immediately following the body text.

Before every ultrasonic thickness measurement considerable surface preparation and scraping was necessary. Before the hand-held and McGyver measurements, and supplemental to the Fury surface preparation/scraping system, a hand-held scraper was used. This scraper was a 6 in. square of 0.25 in. thick steel plate with a sharpened edge welded to 0.5 in. threaded pipe at an angle of approximately 20 degrees. Vigorous scraping to depth was accomplished by adding sections of pipe as needed. The corrosion scale proved to be relatively thick and very adherent.

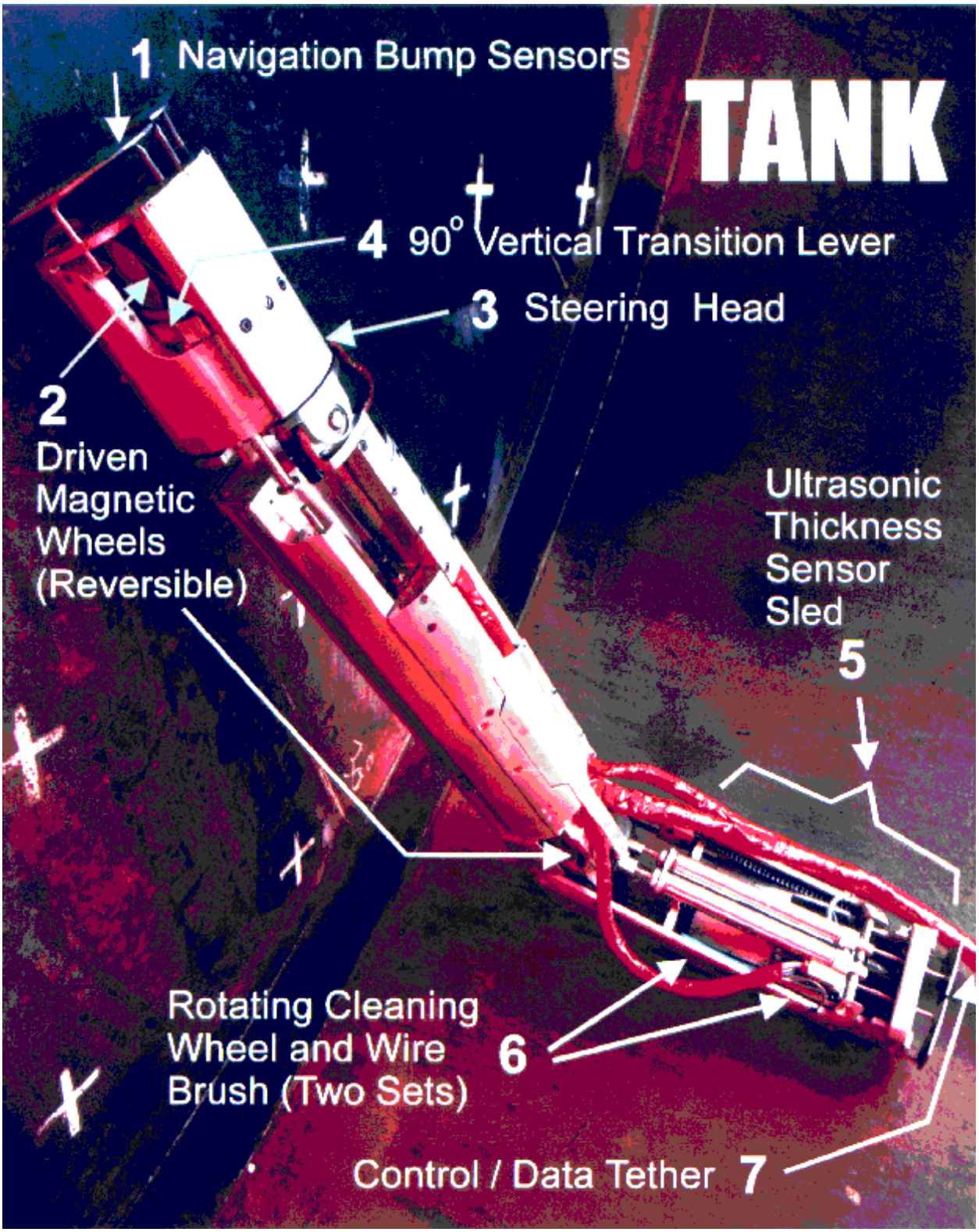

Figure 3. The Fury robot.

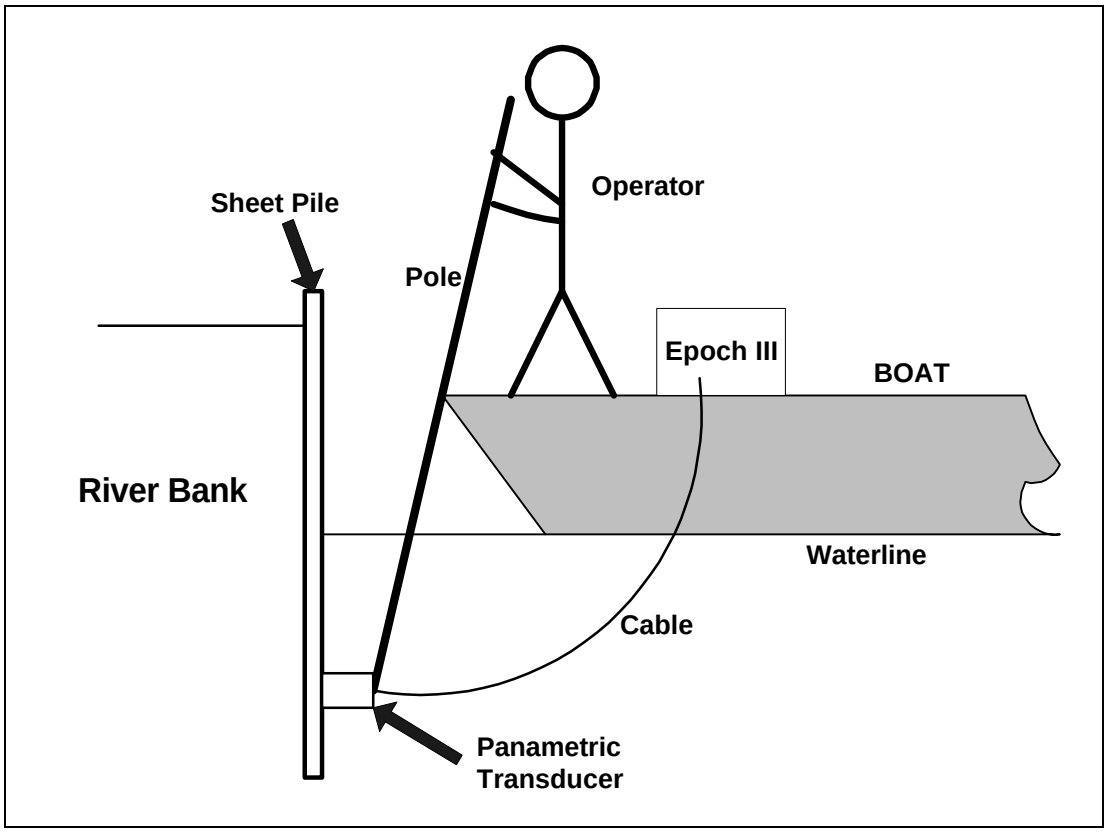

Figure 4. Use of the hand-held acoustic sensor.

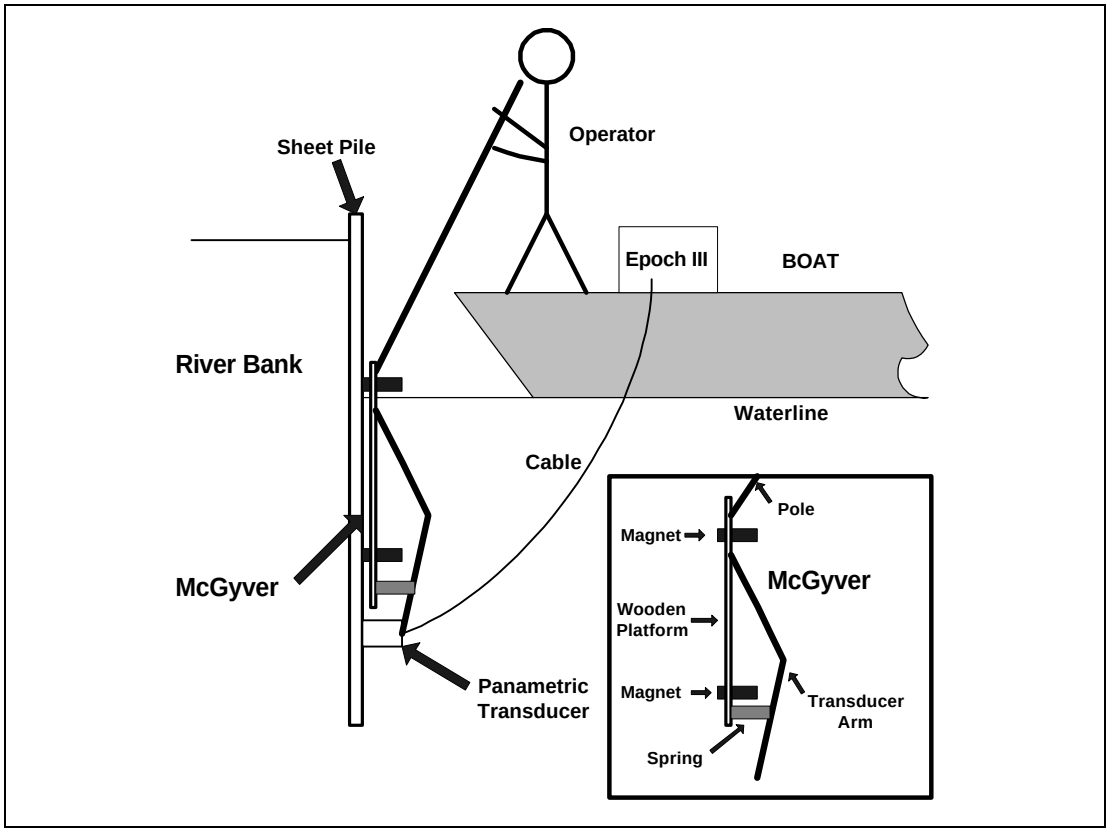

Figure 5. McGyver measuring device.

4 Corrosion Rate Measurements

From the 24 – 28 August 1998, a NACE-certified corrosion engineer was employed to take localized corrosion measurements at the 12 sites where sheet pile thickness was measured. Corrosion rates were measured using the equipment shown in Figure 6, used in conjunction with data analysis software*.

The polarization resistance technique was used to rapidly estimate of the corrosion rate of metal in a solution. In this technique, cell current readings are taken during a very short, slow sweep of the potential. The sweep used in this study was from -20 to +20 mV relative to open circuit potential of the test surface, commonly called "$E_{Open\ Circuit}$" (E_{oc}). Over this range, the current vs voltage curve is generally linear. A linear fit of the data to a standard model yields an estimate of the polarization resistance (R_p) that is then used to calculate the corrosion current (I_{corr}). Using the corrosion current, the corresponding mass loss or corrosion rate of the sheet pile at the test site is then determined (Appendix C).

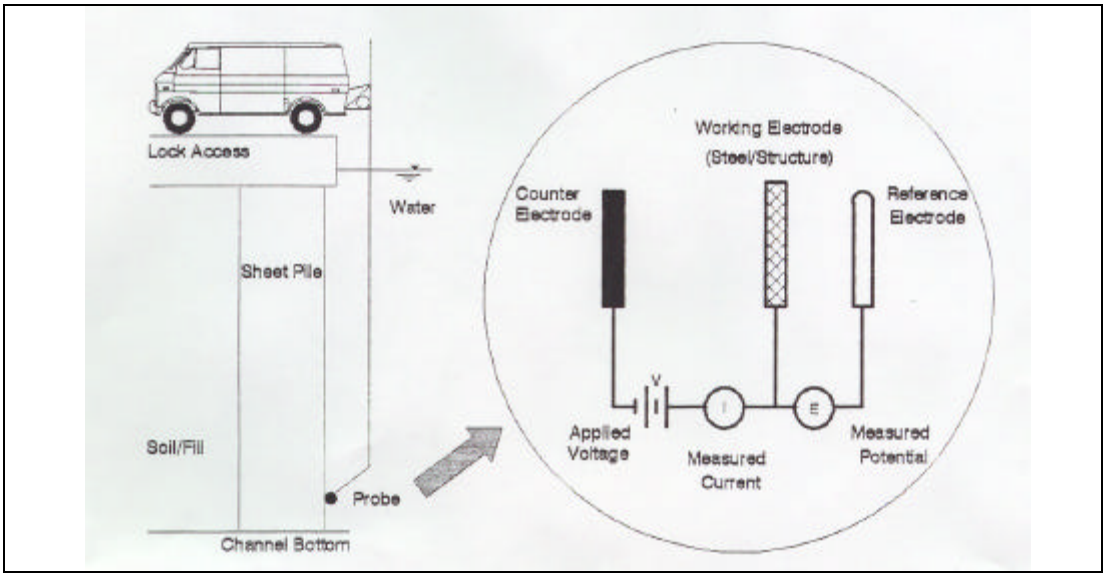

Figure 6. Onsite probe for corrosion rate measurement.

* Gamry CMS 100 Electrochemical Corrosion Testing software and hardware installed on a Gateway P5/133 computer operating under Windows 95.

There are numerous advantages to using the polarization resistance technique. Polarization resistance experiments run very quickly. The scan in a polarization resistance experiment does not appreciably polarize the sample. This minimizes changes in the surface of the sample caused by the test itself, which is especially important for long-term monitoring. Furthermore, this technique facilitates re-running the scans when data acquisition during a particular test was disturbed by external sources. There are a couple of disadvantages to using the polarization resistance technique. The corrosion rate calculation requires the tester to provide kinetic parameters (Beta slopes) that must be estimated or obtained from another type of experiment. In this test, the Beta slope value used for both the anodic and cathodic slopes was 120 mV/Decade. This value is the one most commonly used in aqueous electrolytes and is well accepted as a very close approximation of the actual slope(s) in the Cuyahoga River water environment. Under laboratory conditions, the result of a polarization resistance calculation may be somewhat less accurate than the corrosion rate calculated from Tafel data. Unfortunately, Tafel tests require considerably longer time to run (typically more than 1 hour), and any change in condition during this test will distort or even completely invalidate the results. During this study, a number of Tafel scans were attempted but each time external noise from passing ships, spurious electrical signals, etc., significantly distorted the data and no analysis could be made of the data obtained during any of these scans. Analysis of the curve can yield the corrosion potential, corrosion current, and corrosion penetration rate.

ASTM Standard G-59, *Practice for Conducting Potentiodynamic Polarization Resistance Measurements,* contains additional useful information about polarization resistance measurements. Details of the measurement procedure and the polarization resistance plots are given in Appendix C.

A total of 31 polarization resistance (PR) and 5 Tafel scans were performed on submerged portions of the steel sheet pile along the Cuyahoga River. These scans were conducted at 10 different sites that corresponded to locations where ultrasonic thickness measurements were obtained.

As noted, none of the Tafel scans provided accurate, useful data. However, 23 of the 31 polarization resistance scans were completed successfully and provided meaningful results for the current *in-situ* corrosion rates occurring on the sheet pile water-side surfaces. A summary of the corrosion rate data is given in Table 1.

Table 1. Corrosion rate analysis data.

Site	Ecorr (-mV)	Icorr (Amps/cm2)	Rp (Ohms/cm2)	Corrosion Rate (mils/Year)	Corrosion Rate (inches/Year)
1	365.3	1.48E-06	1.76E+04	1.844	0.001844
2	637.6	2.58E-06	1.01E+04	3.215	0.003215
2	605.4	9.67E-11	2.70E+08	0	0
2	640.4	1.04E-05	2.50E+03	12.98	0.01298
Near 2	410.4	3.91E-03	6.66E+00	27.067	0.027067
Near 2	509	4.18E-05	6.24E+02	51.982	0.051982
Near 2	601.8	1.29E-05	2.02E+03	16.052	0.016052
3	404.7	3.42E-05	7.62E+02	1.082	0.001082
3	426.2	5.24E-06	4.97E+03	6.522	0.006522
3	601.8	2.79E-05	9.34E+02	34.75	0.03475
4	384.6	8.63E-06	3.02E+03	10.744	0.010744
4	573.7	1.53E-05	1.71E+03	18.977	0.018977
4	584.7	4.07E-06	6.40E+03	5.071	0.005071
5	353.5	3.21E-06	8.13E+03	3.992	0.003992
6	621.6	2.44E-06	1.07E+04	3.043	0.003043
6	508	6.52E-06	4.00E+03	8.113	0.008113
7	541	1.74E-06	1.50E+04	0.055	0.000055
7	550.6	8.77E-06	2.97E+03	10.92	0.01092
8	432.2	8.81E-06	2.96E+03	10.963	0.010963
11	553.4	3.85E-06	6.77E+03	4.795	0.004795
12	676.9	6.49E-06	4.01E+03	8.086	0.008086
12	589.9	1.40E-06	1.87E+04	1.739	0.001739
12	588	1.35E-06	1.94E+04	1.675	0.001675
Minimum	353.5	9.67E-11	6.66E+00	0	0
Maximum	676.9	3.91E-03	2.70E+08	51.98	0.05198
Average	527.64	3.21E-04	2.16E+07	11.83	0.01183
Std. Dev.	98.47	8.14E-04	5.62E+07	12.56	0.01256

In addition, resistivities were measured for both water and soil. The water resistivity was found to be 1010 ohm-cm. The soil resistivity was measured using the Werner 4-pin method with intermediate values inferred using the Barnes layering technique. Appendix D contains full details of measured values. At both the 5 ft and 10 ft depth, a value of 5050 ohm-cm was found. This is considered only moderately corrosive, especially when compared to the water side. Additional water chemistry data from the Ohio Environmental Protection Agency are included in Appendix D.

5 Video Inspection of Sheet Pile

While thickness and corrosion rate measurements were being performed, a videotape of the condition of the sheet pile below the water surface was recorded at 1 ft intervals. Although the Cuyahoga's lack of water clarity made filming difficult, a field-adapted device fitted to the front of the camera allowed for some marginally useful video footage to be taken. Both visible-color and infrared cameras were used. Figures 7, 8, and 9 show screen images of the captured video. Aside from indicating the degree of zebra mussel infestation, video or still images have considerably less utility for inspection and assessment compared to thickness and corrosion rate measurements.

Figure 7. Waterline video capture of sheet pile at Site 1.

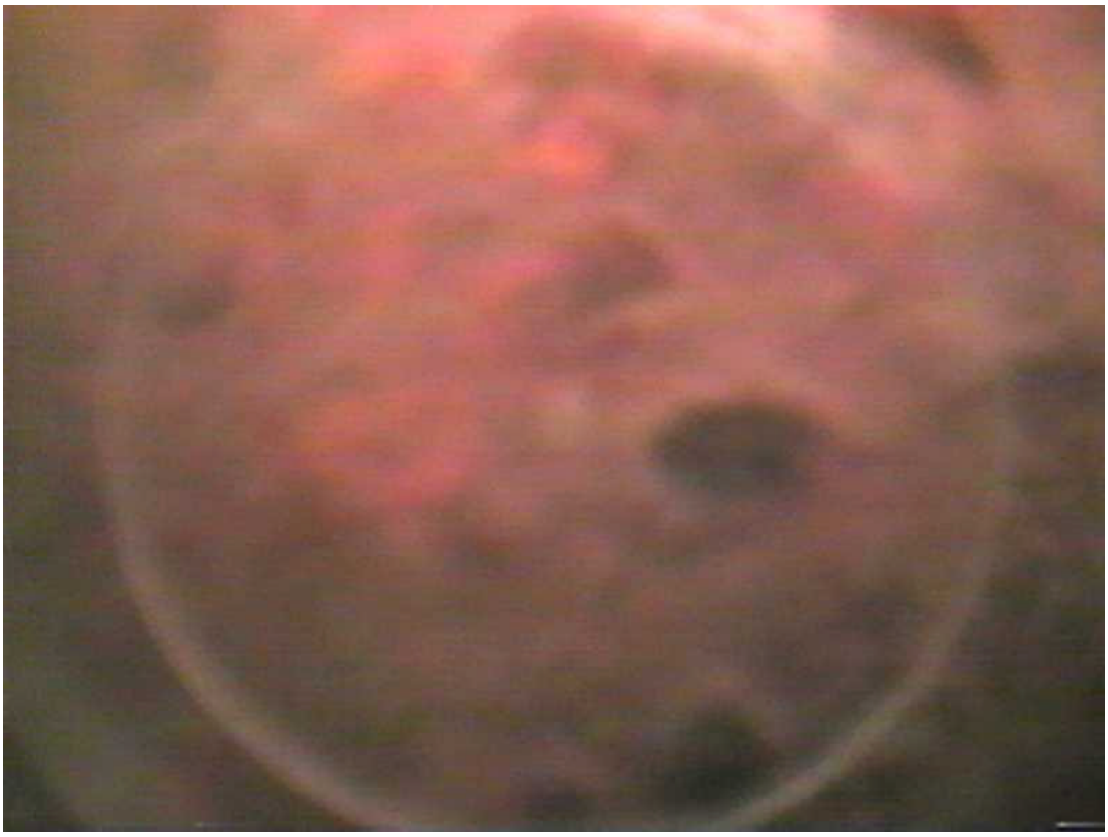

Figure 8. Video capture of Site 1 at 10 ft below waterline.

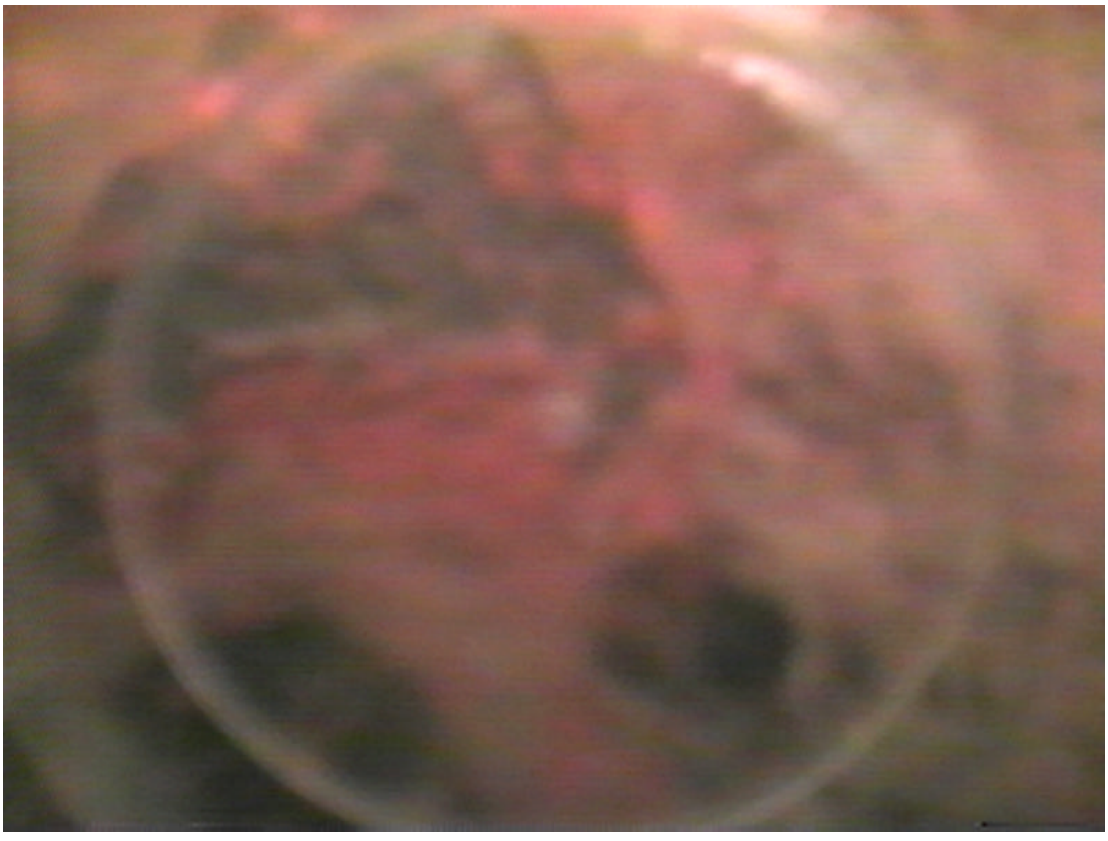

Figure 9. Video capture of Site 1 at 25 ft below waterline.

6 Discussion

The data acquired from the 12 surveyed sites were entered into a spreadsheet and plotted. The results from each site are plotted on a graph, with the data tables and plots included as attachments to this document.

Different thickness values measured at a specific depth do not necessarily represent error or anomaly. It is more likely that the measurements were taken at different horizontal locations at the same depth, and in fact represent actual different wall thicknesses.

Although this work was the first time Fury was adapted for *in-situ* corrosion assessment of sheet pile, the cost was still comparable to a four-person dive crew. With the experience gained in dealing with tough, adherent scale and very cloudy water, and with further technical adaptations of the Fury system for this application, it seems certain that the cost of robotic inspection and assessment can be driven significantly lower.

Zebra mussels are present in Lake Erie, but they were not found in great numbers at any site surveyed except for Site 12. Since Site 12 is closest to Lake Erie, a reasonable conjecture is that the encroachment of zebra mussels will proceed inland, assuming adequate initial environmental conditions for growth and reproduction. Although the rate of this migration is unknown, it is likely to adversely affect the corrosion rate of installed sheet pile. Experience at Black Rock Lock in Buffalo, NY, suggests that zebra mussels increase the corrosion rate by a factor of 5 compared to the rate in noninfested water. On the plus side, as filter feeders, the Zebra mussels are likely to have a positive effect on the clarity of Cuyahoga River water. It seems prudent therefore, to verify both the encroachment patterns and accelerated corrosion rates before considering available options for control.

It can reasonably be assumed that the water-side corrosion will typically dominate over soil-side corrosion with respect to the sheet pile deterioration.

Based on the data from all 23 polarization resistance scans, the average corrosion rate measured was slightly less than 12 mils per year with a standard deviation of 12.5 mils per year. Given the 500 mil thickness of the sheet pile typi-

cally used along the river, time to perforation of the pile due to water-side corrosion would typically occur approximately 40 years after installation.

However, the variation in the rates measured suggests that locations with more aggressive environments could experience failure much sooner. Given the relatively few measurements and the inherent and unavoidable uncertainties associated with the polarization resistance technique, no single measured value alone should be considered as an accurate value. Instead, taken together, a corrosion rate of 11.8 mils per year should be considered as representative river-wide.

On a structures and/or planning basis, the time to perforation may not be of greatest concern. Table 2 summarizes the results of projecting the time needed to reach 50, 30, and 10 percent of the original thickness for the 12 sites. A consistent and ongoing rate of 11.8 mils per year is assumed for all sites. An average of the current measured thicknesses is used as a starting value for each site. The maximum and minimum values are the result of starting with a thickness of plus or minus one standard deviation. Figures 10 – 22 follow the same approach, but instead represent a continuous presentation of the corrosion process. Table 3 gives estimated dates of sheet pile construction for each measurement site.

Table 2. Life-cycle projection table for the sheet pile.

Site	Type of Sheet pile	Ave. Thick (in)	STD (in)	50% Max (yrs)	50% Min (yrs)	50% Ave (yrs)	30% Max (yrs)	30% Min (yrs)	30% Ave (yrs)	10% Max (yrs)	10% Min (yrs)	10% Ave (yrs)
1	Cold	0.3533	0.1	20.33	0.33	10.33	30.33	10.3	20.3	40.33	20.3	30.3
2	Cold	0.379	0.04	16.9	8.9	12.9	26.9	18.9	22.9	36.9	28.9	32.9
3-Web	Hot	0.28	0.094	18.65	0	9.25	26.15	7.35	16.8	33.65	14.9	24.3
4-Flange	Hot	0.32	0.092	16.2	0	7	26.2	7.8	17	36.2	17.8	27
5-Web	Hot	0.233	0.119	16.45	0	4.55	23.95	0.15	12.1	31.45	7.65	19.6
5-Flange	Hot	0.39	0.007	14.7	13.3	14	24.7	23.3	24	34.7	33.3	34
6-Web	Hot	0.251	0.054	11.75	0.95	6.35	19.25	8.45	13.9	26.75	16	21.4
7-Web	Hot	0.306	0.043	16.15	7.55	11.85	23.65	15.1	19.4	31.15	22.6	26.9
8-Web	Hot	0.306	0.048	16.65	7.05	11.85	24.15	14.6	19.4	31.65	22.1	26.9
9-Flange	Hot	0.301	0.118	16.9	0	5.1	26.9	3.3	15.1	36.9	13.3	25.1
10-Flange	Hot	0.32	0.075	14.5	0	7	24.5	9.5	17	34.5	19.5	27
11-Flange	Hot	0.234	0.109	9.3	0	0	19.3	0	8.4	29.3	7.5	18.4

Table 3. Estimated dates of construction by site.

1940s	1950s	1960s	1970s	1980s	1990s
Sites 2, 4, 9 Site 10 –1942 Sites 12,8 –1945 Site 5 –1948 Site 11 -1949	Site 7	Site 6	None	None	Sites 1,3 –1990

Note: Due to the lack of information, years for Sites 2, 4, 6, 7, and 9 have been estimated based on known ages of nearby bulkheads on the same property.* Site 2 appeared to be much more recent than 1940s.

It must be remembered that while the land-side corrosion rates will usually be substantially lower than for water-side corrosion, site-specific factors may reverse this. For example, Site 4 has major subsidence behind the pile. Coal coke had been stored in the immediate area. This coal coke has extremely low resistivity and is probably acidic. The leaching of this material into the soil side backfill immediately behind the pile will substantially increase the land-side corrosion rate causing much earlier failure than at other sites.

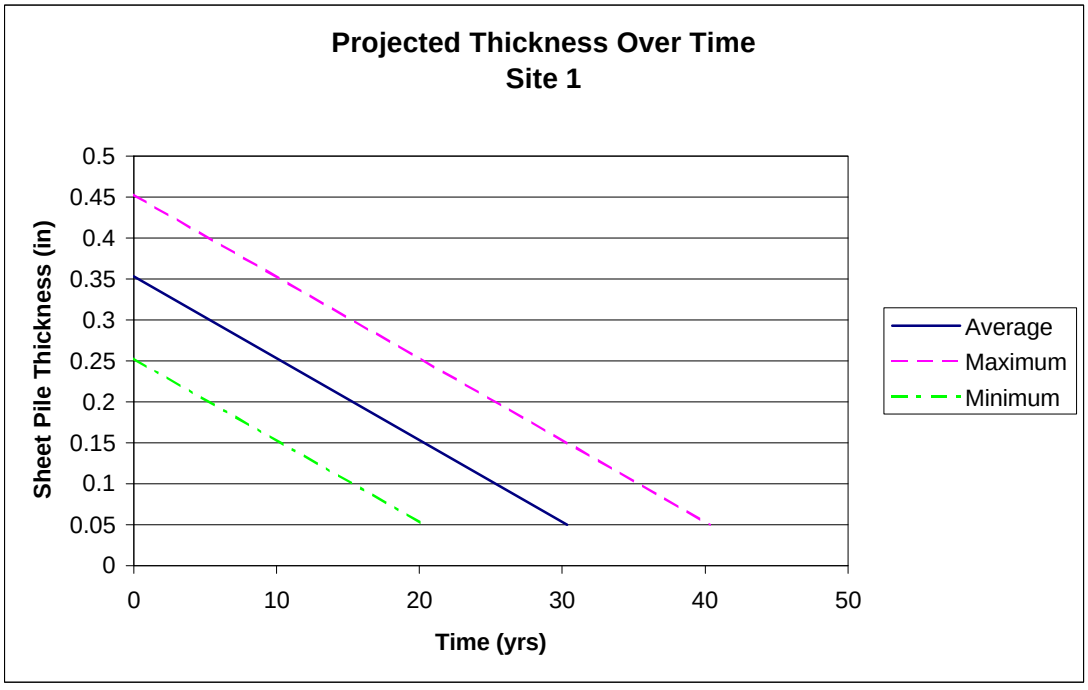

Figure 10. Site 1 projected thickness over time.

* Personal communication from Frank T. Lewandowski, 22 January 1999.

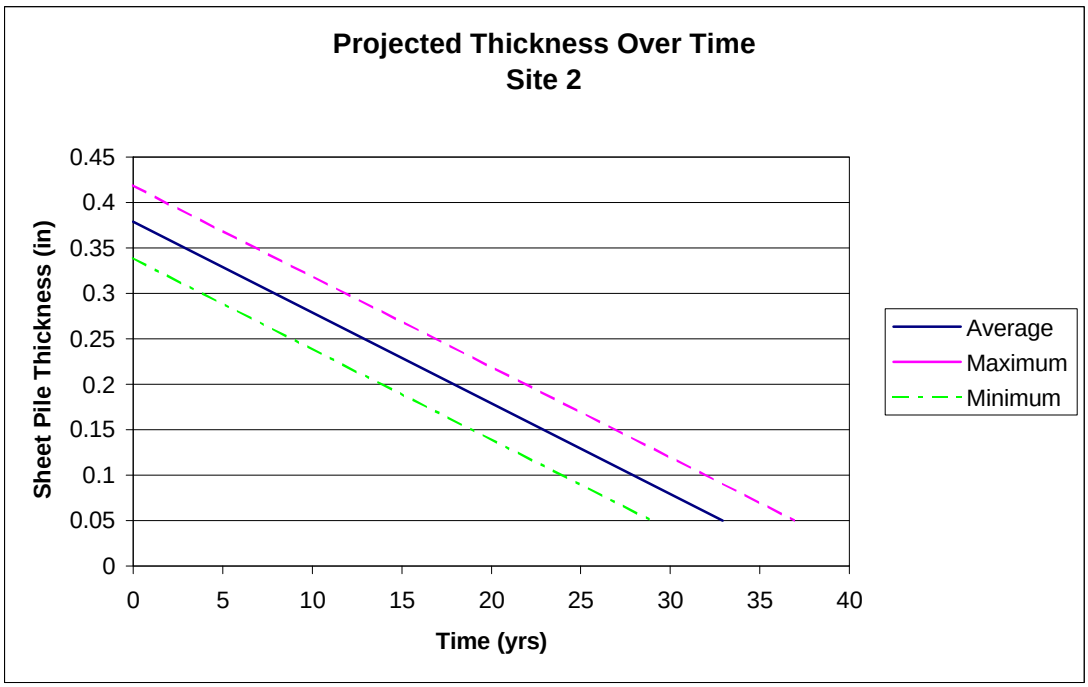

Figure 11. Site 2 thickness projected over time.

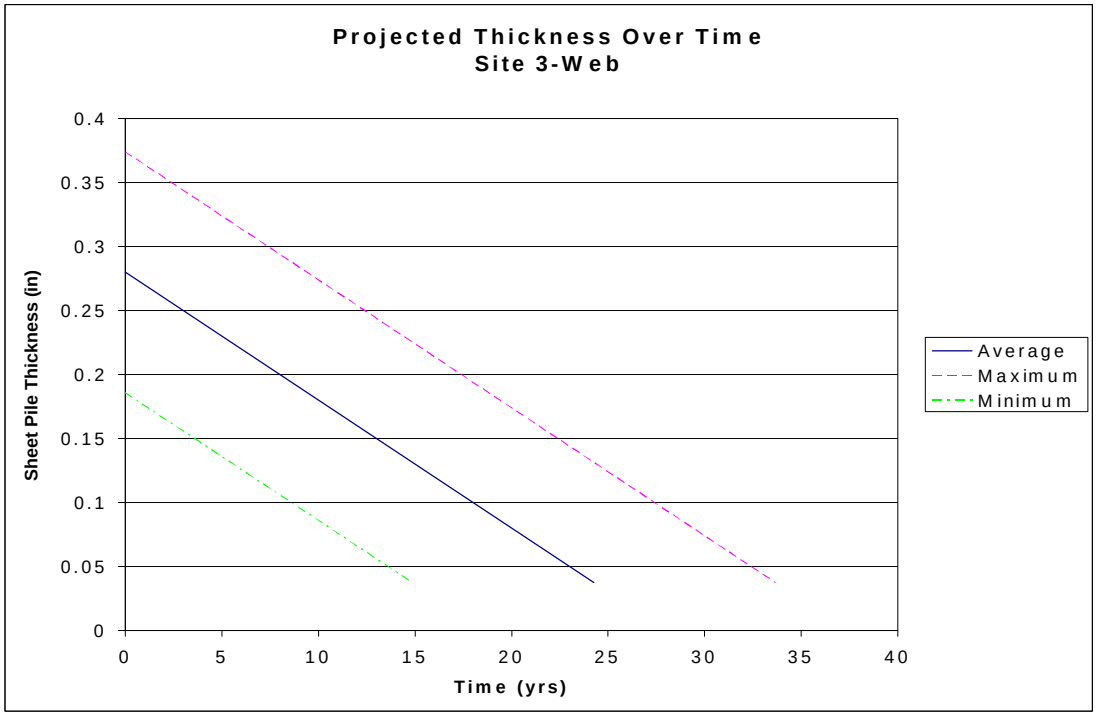

Figure 12. Site 3 web thickness projected over time.

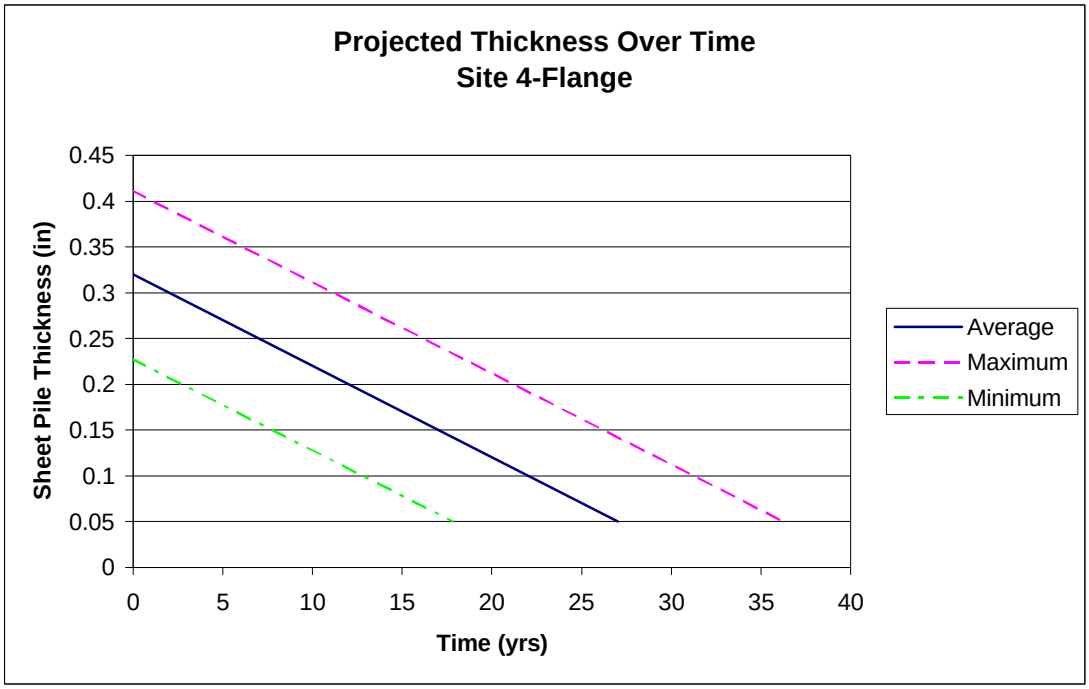

Figure 13. Site 4 flange thickness projected over time.

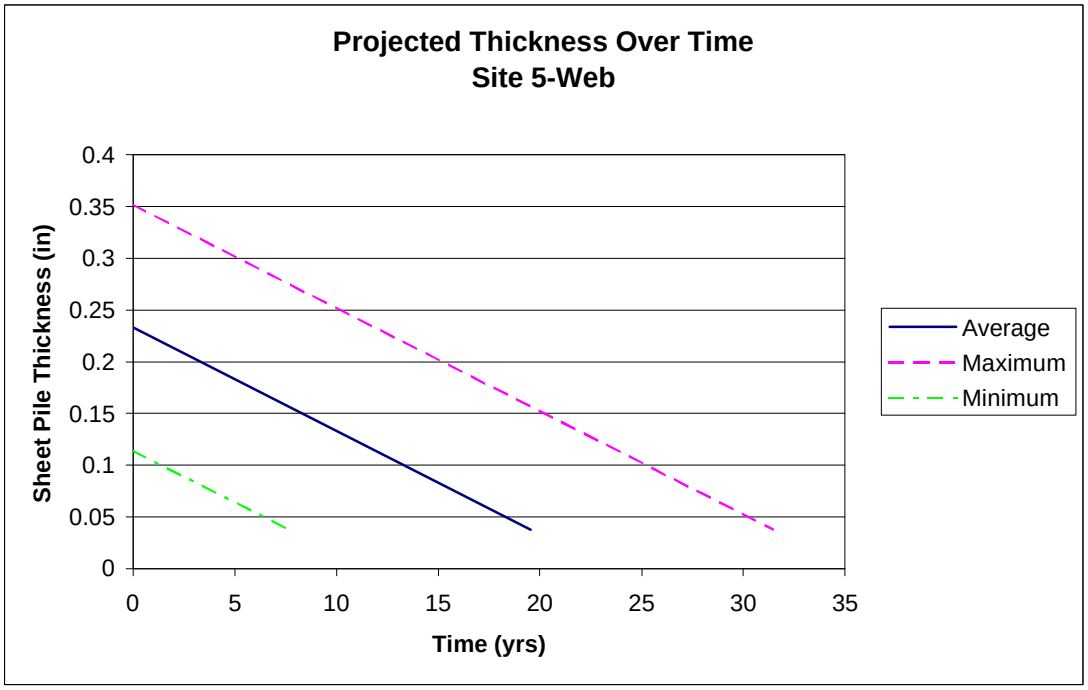

Figure 14. Site 5 web thickness projected over time.

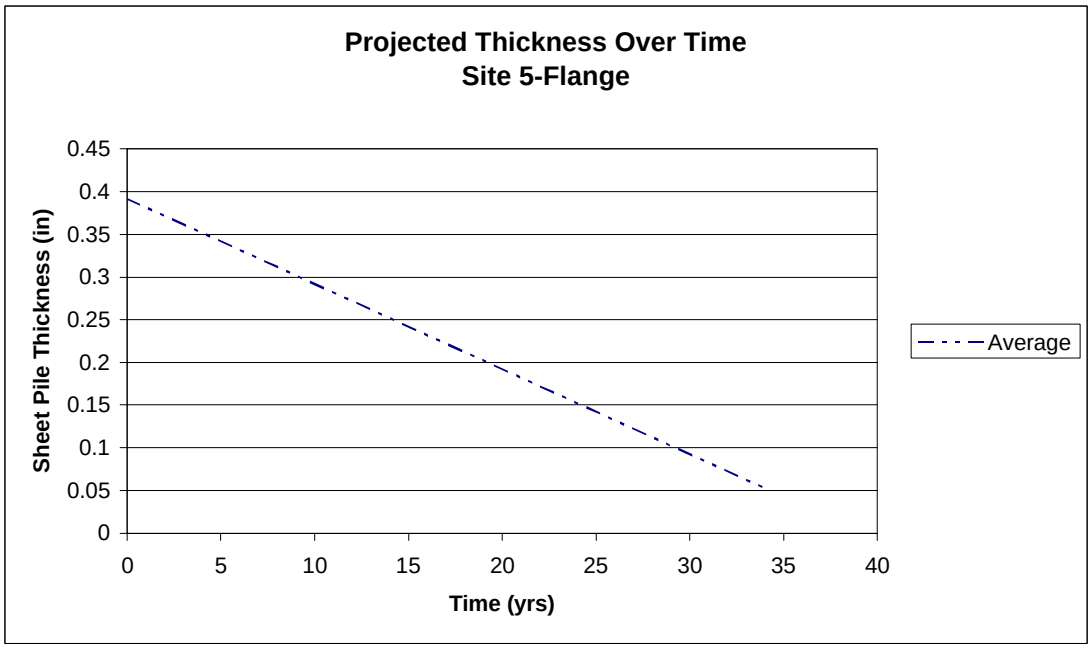

Figure 15. Site 5 flange thickness projected over time. Note: There were too few reliable measurements to determine a valid max/min range in this case.

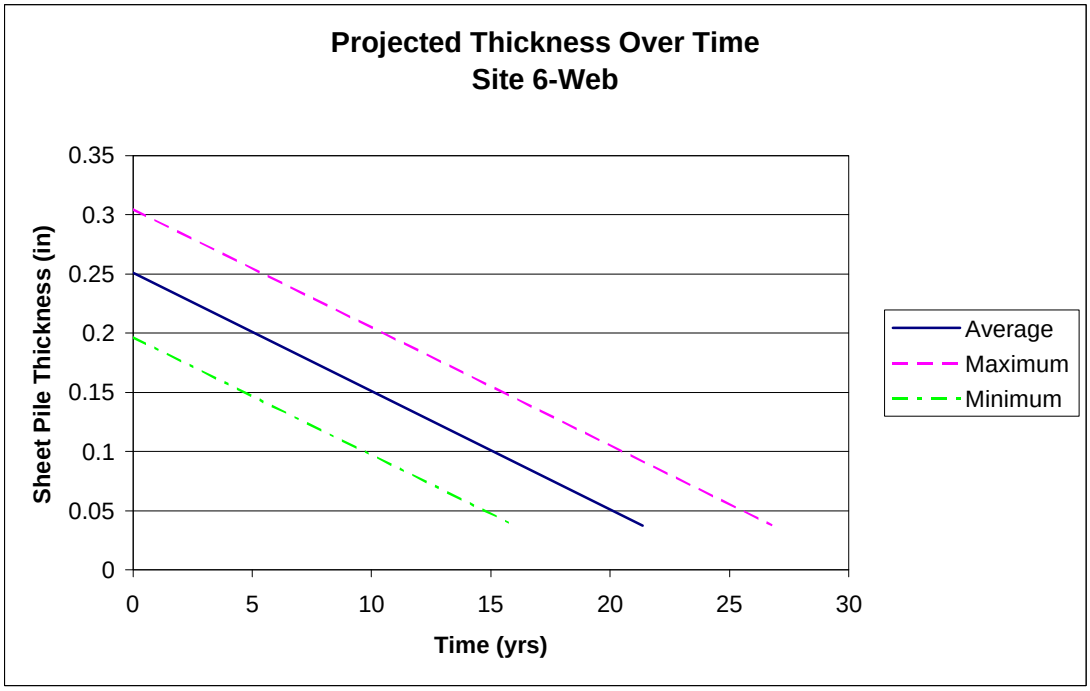

Figure 16. Site 6 web thickness projected over time.

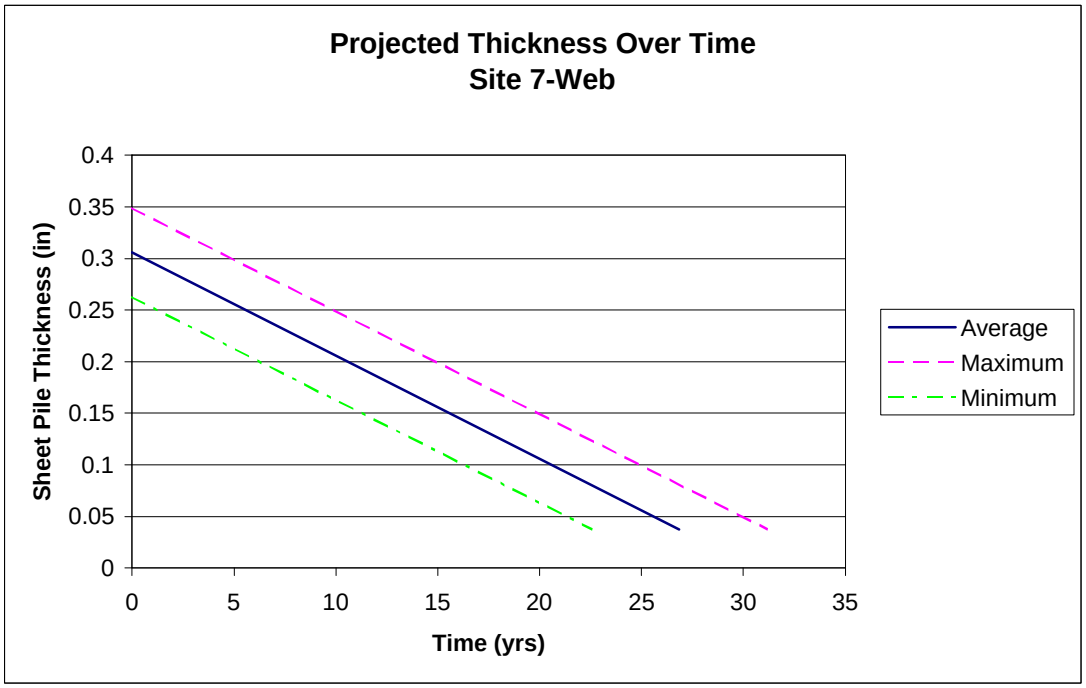

Figure 17. Site 7 web thickness projected over time.

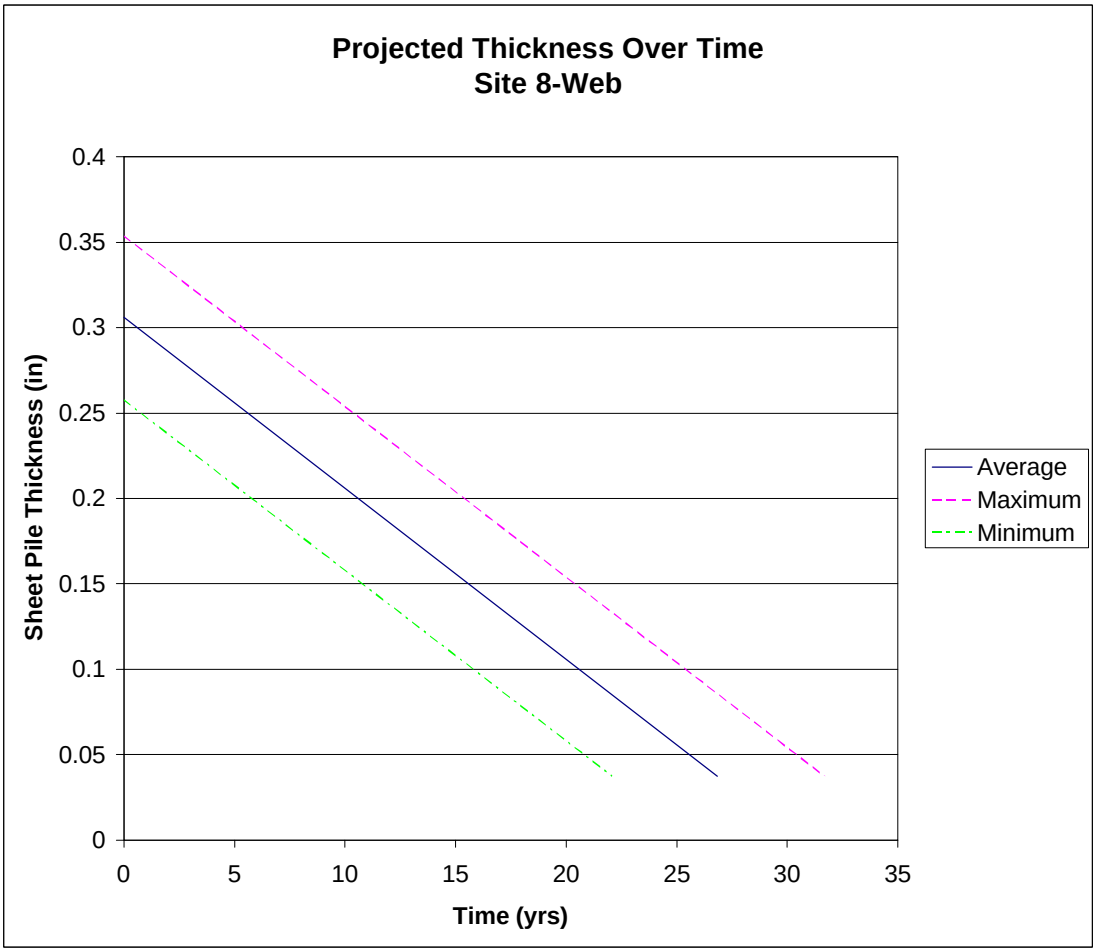

Figure 18. Site 8 web thickness projected over time.

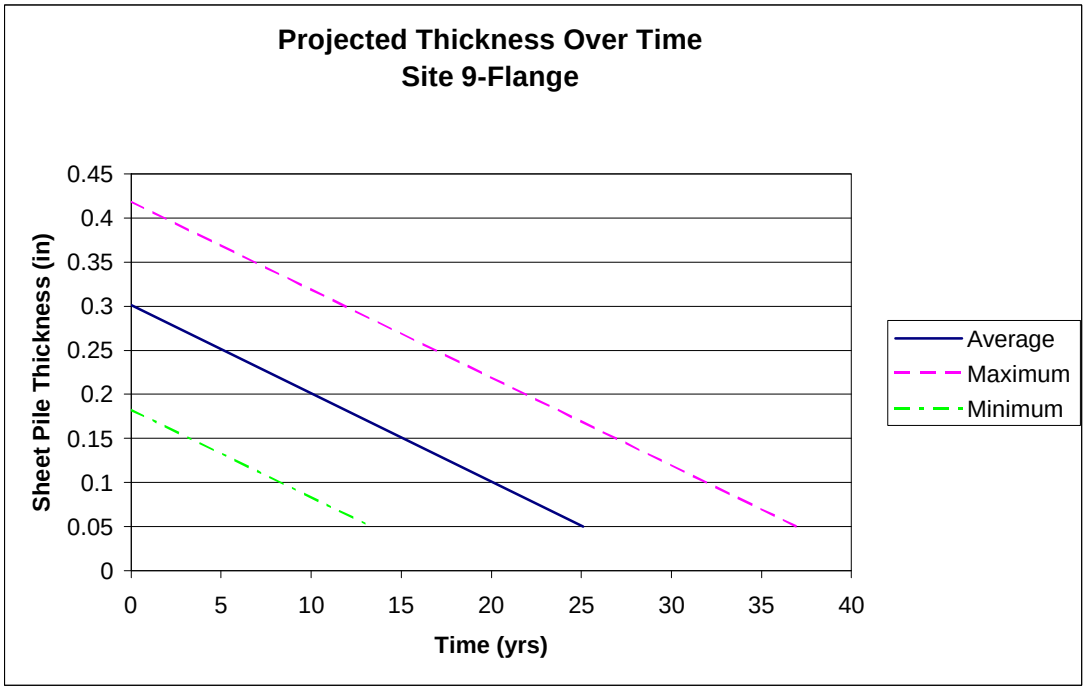

Figure 19. Site 9 flange thickness projected over time.

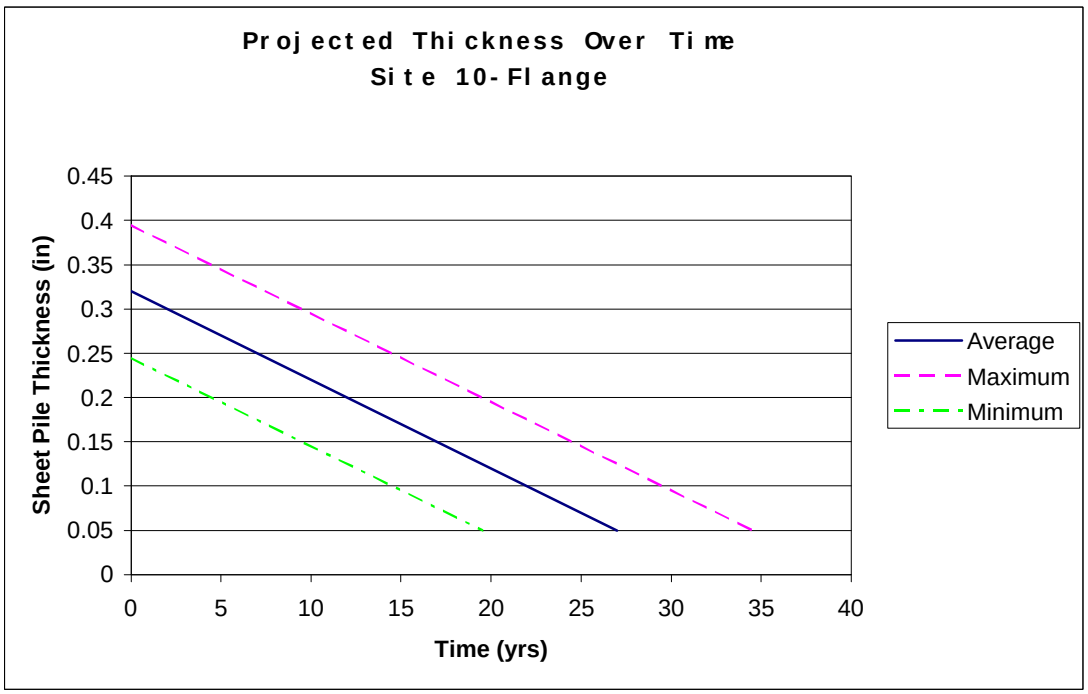

Figure 20. Site 10 flange thickness projected over time.

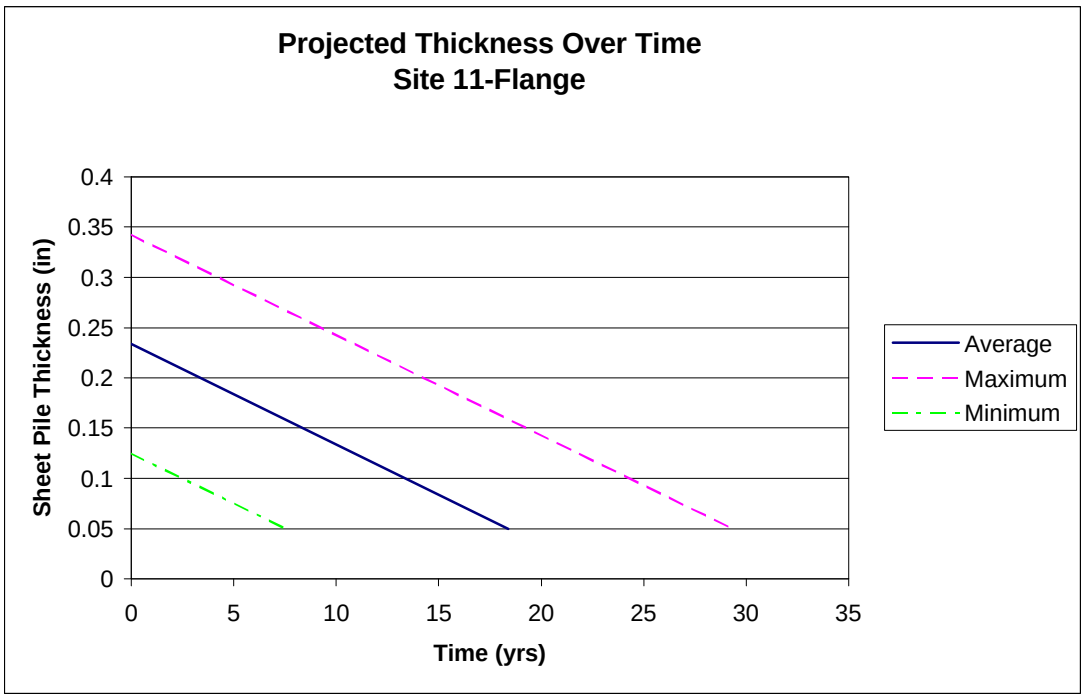

Figure 21. Site 11 flange thickness projected over time.

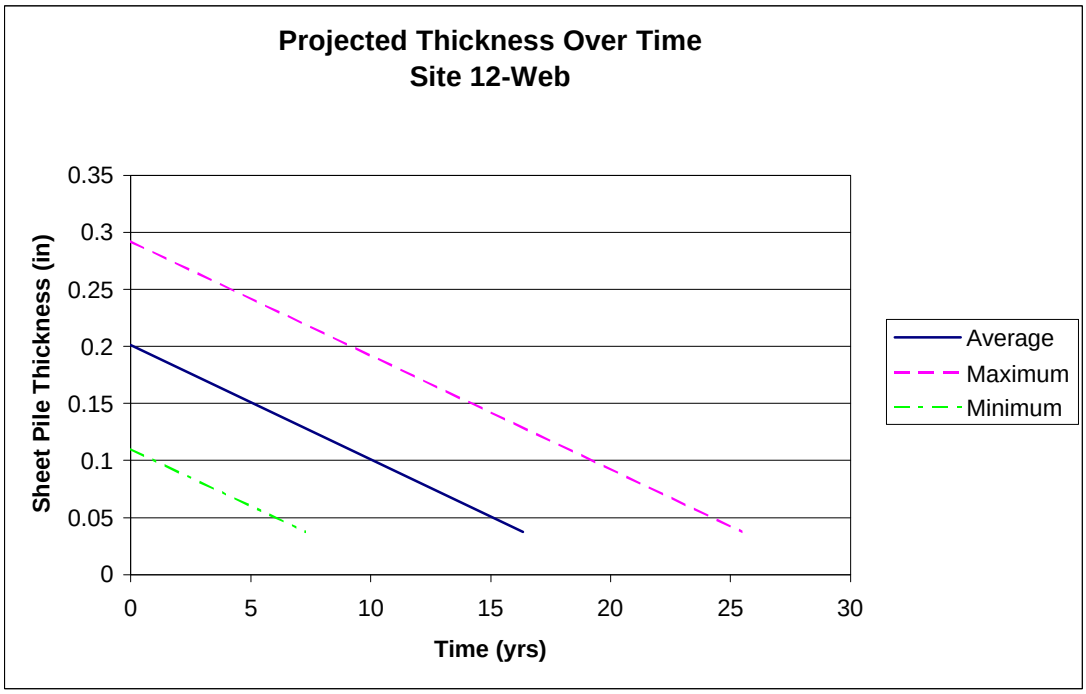

Figure 22. Site 12 web thickness projected over time.

7 Summary and Recommendations

Summary

Thickness and corrosion rate measurements were made to obtain quantitative data pertaining to the current underwater condition of the sheet pile at 12 specified sites along the Cuyahoga and Old Rivers. Thickness measurements were made both by the Fury remotely controlled robotic inspection system and by manual acoustic sensing technology. Based on limited data samples collected in this study, a bounded, steady-state projection of future sheet pile condition was made for each site.

During this study zebra mussels were found along the river, with the largest populations located near the mouth of the river and Lake Erie. Because previous studies have indicated that there may be a positive linkage between corrosion rates and degree of zebra mussel infestation, the rate of corrosion measured in this study may accelerate if zebra mussel colonies move up river as anticipated. In such a case, the projected sheet pile thicknesses reported here would be too large, and any given percentage of original material thickness would be reached sooner than projected here.

Recommendations

Based on the results of this study, the following recommendations are offered:

- A structural analysis on reduced section modulus should be conducted to determine the overall average reduced thickness at which failure may reasonably be expected.
- Based on the projected time to failure, property owners should be notified in advance, and replacement should be scheduled before the bulkhead fails.
- Additional measurements should be made at the 12 sites in order to improve the statistical reliability of the current findings.
- The encroachment rate of zebra mussels into the Cuyahoga should be verified.
- Verify the linkage between zebra mussel infestation and accelerated corrosion rates before implementing control methods.

References

ASTM Standard G-59, *Practice for Conducting Potentiodynamic Polarization Resistance Measurements*.

Barnes, H.E., *Electrical Survey Detects Underground Rock*, Pipeline Industry, April 1959.

Chaker, Victor, "Simplified Method for the Electrical Soil Resistivity Measurement", Underground Corrosion Symposium, sponsored by ASTM Committee G-1, Williamsburg, VA, 26-27 November 1979. ASTM Publication Code Number 04-741000-27, Philadelphia, PA, 1981.

Claudi, Renata and Gerald L. Mackie; *Practical Manual for Zebra Mussel Monitoring and Control* (CRC Press Inc., Boca Raton FL, 1994).

Evans, Ulrick R., The Corrosion and Oxidation of Metals: Scientific Principles and Practical Applications. Edward Arnold Publishers Ltd, London, 1960.

Greimann, Lowell, and James Strecker, *Maintenance and Repair of Steel Pile Structures*, CERL Technical Report (TR) REMR-OM-9 (U.S. Army Construction Engineering Research Laboratory, December 1990, ADA 231916).

Marsh, Charles P., Amer Siddique, and Vincent F. Hock, "Fury: A Remote Underground Storage Tank Inspection/Assessment System," *Proceedings of the 2d Tri-Service Environmental Technology Workshop*, 10 – 12 June 1997, St. Louis, MO (U.S. Army Environmental Center).

Public Law 104-303, The Water Resources Development Act of 1996, Section 438, "Cuyahoga River, Ohio" (12 October 1996).

Race, Timothy D. and Mark A. Kelly, "Controlling Zebra Mussels with Coatings," *Journal of Protective Coatings and Linings*, Vol. 13, No. 12, Dec. 1996; pp60-72.

URS Greiner, Inc., *Phase 1 Report: Cuyahoga River Bulkhead Study, Cleveland, Ohio*, Contract DACW49-96-D-005, Work Order #6 (Army Engineer District Buffalo, January 1998).

Wenner, Frank, "A Method of Measuring Earth Resistivity," NBS Bulletin No. 12 (469), National Bureau of Standards.

Figures

The plots use the following lines to represent the original thickness of the sheet pile and the standard deviation limits of the measurements:

Original Thickness for the Flange or Web Measurements

Average Thickness for the Flange or Web Measurements

Standard Deviation Limits for Cold Rolled sheet Pile and the Flange Measurements for Hot Rolled Sheet Pile

Standard Deviation Limits for Hot Rolled Sheet Pile Web Measurements

Original and average thickness lines for hot rolled sheet pile are labeled as either flange or web measurements. For cold rolled sheet pile, the original web and flange thicknesses are equivalent.

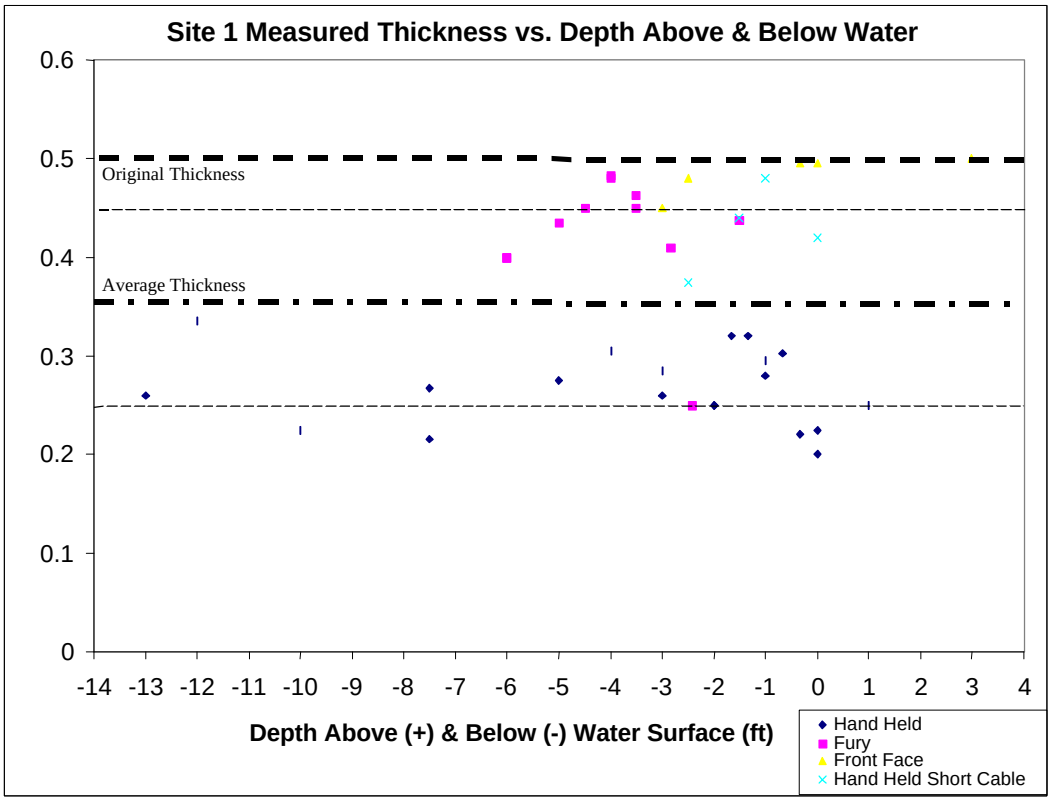

Figure 23. Site 1 thickness measurements.

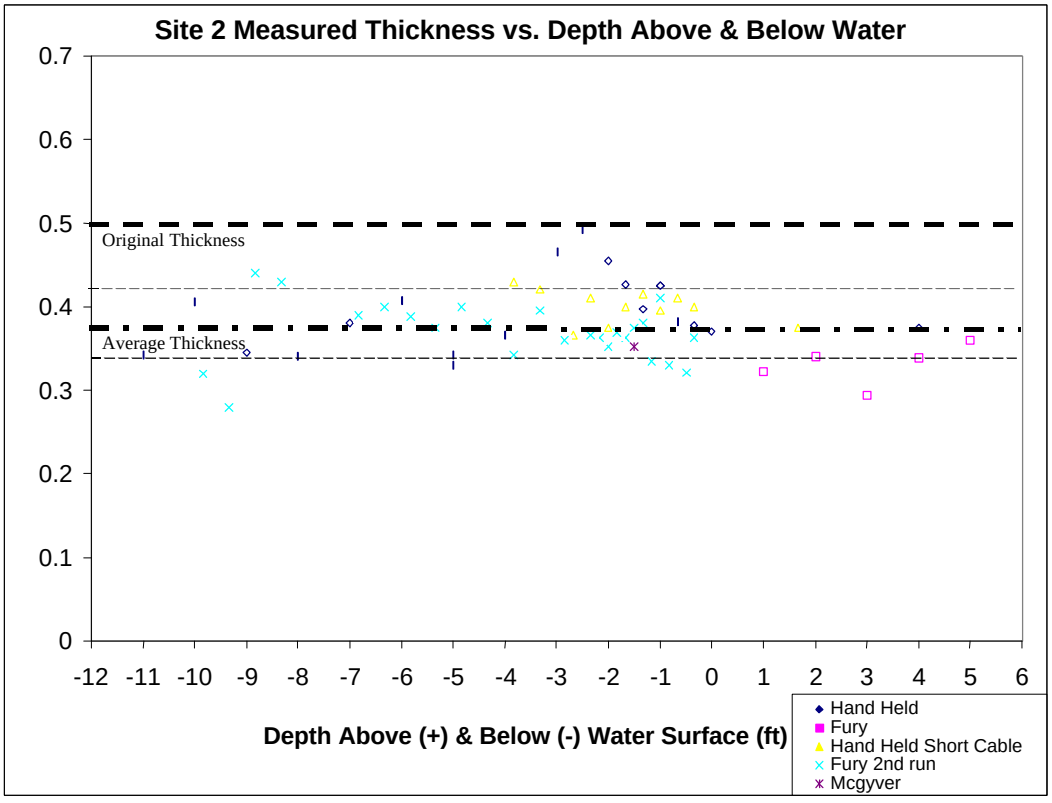

Figure 24. Site 2 thickness measurements.

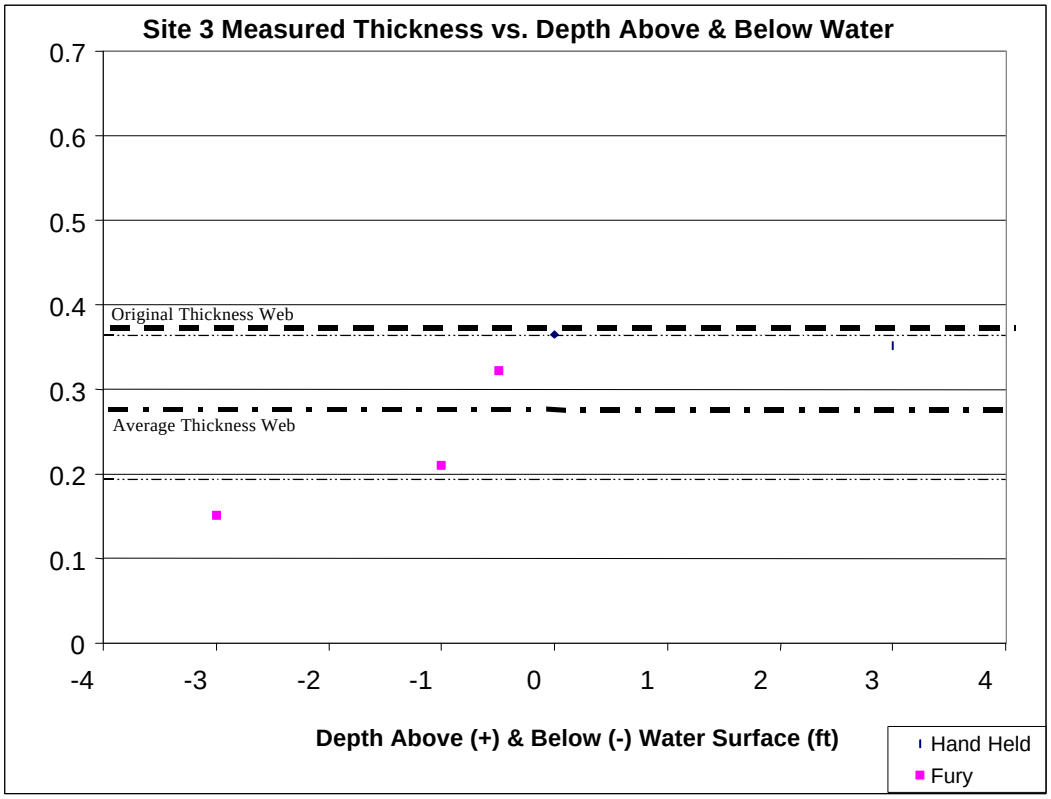

Figure 25. Site 3 thickness measurements.

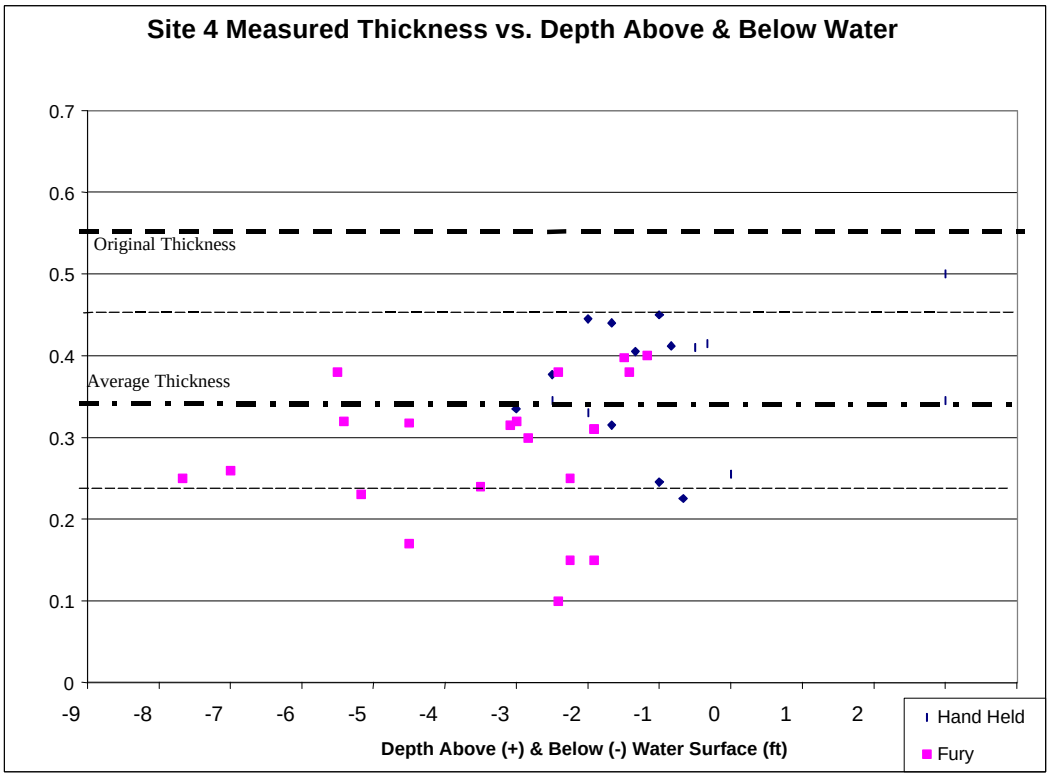

Figure 26. Site 4 thickness measurements.

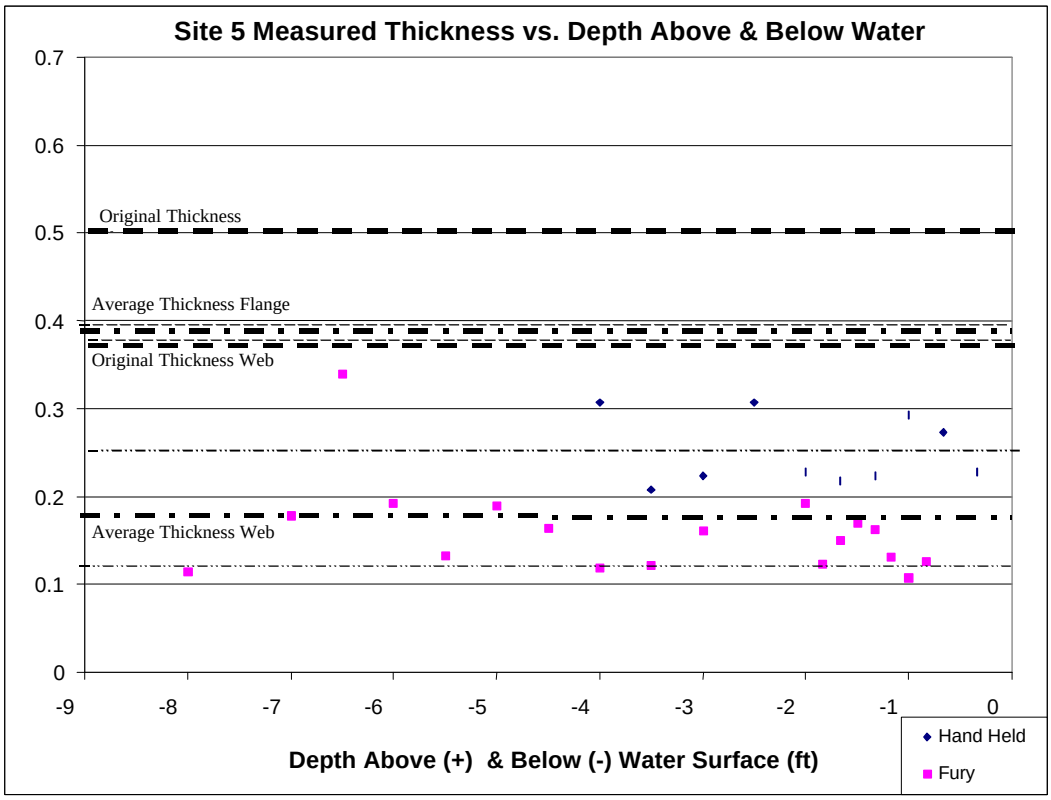

Figure 27. Site 5 thickness measurements.

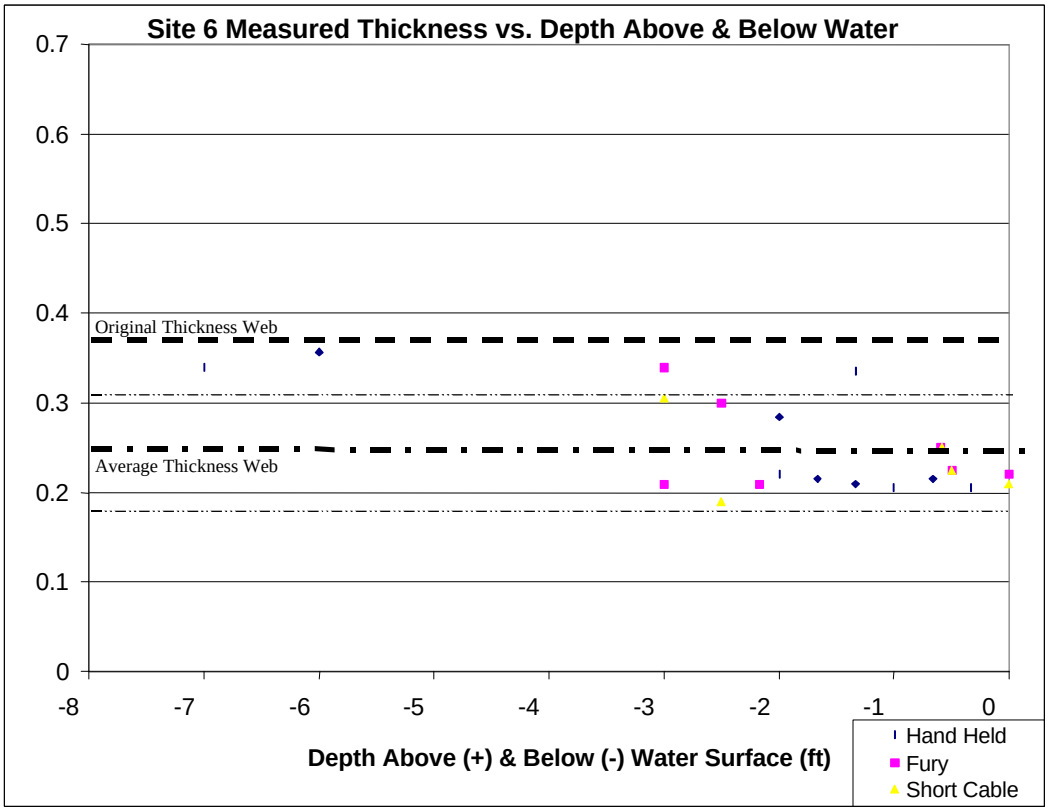

Figure 28. Site 6 thickness measurements.

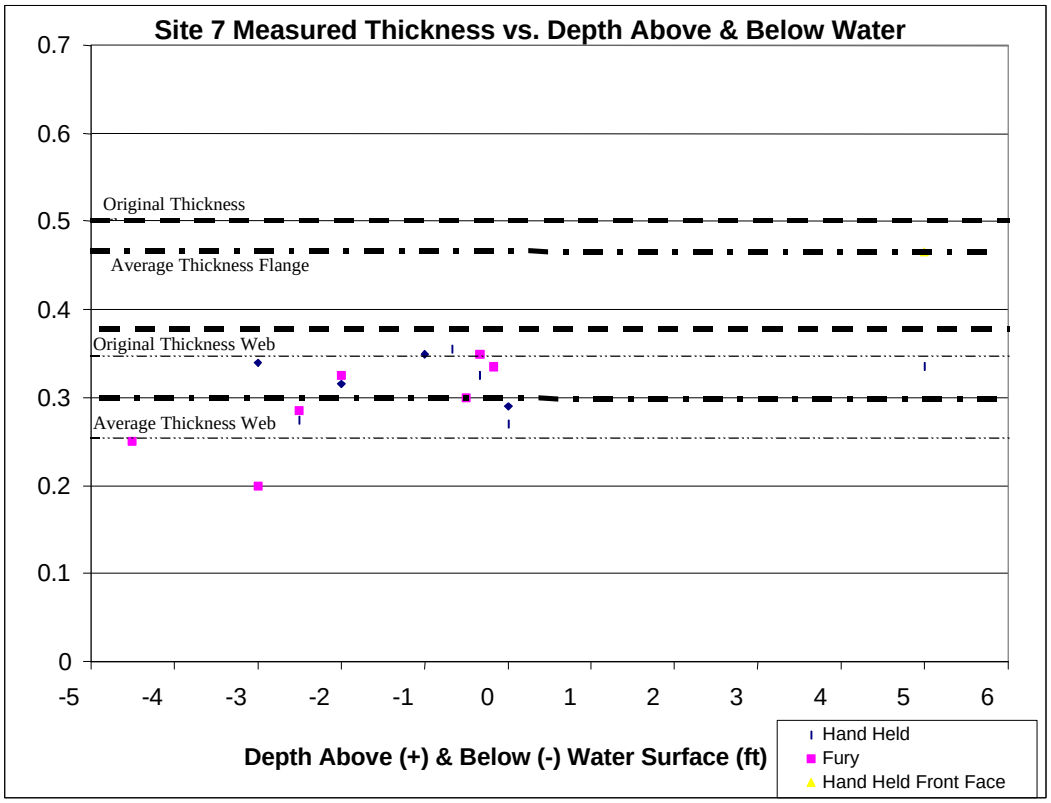

Figure 29. Site 7 thickness measurements.

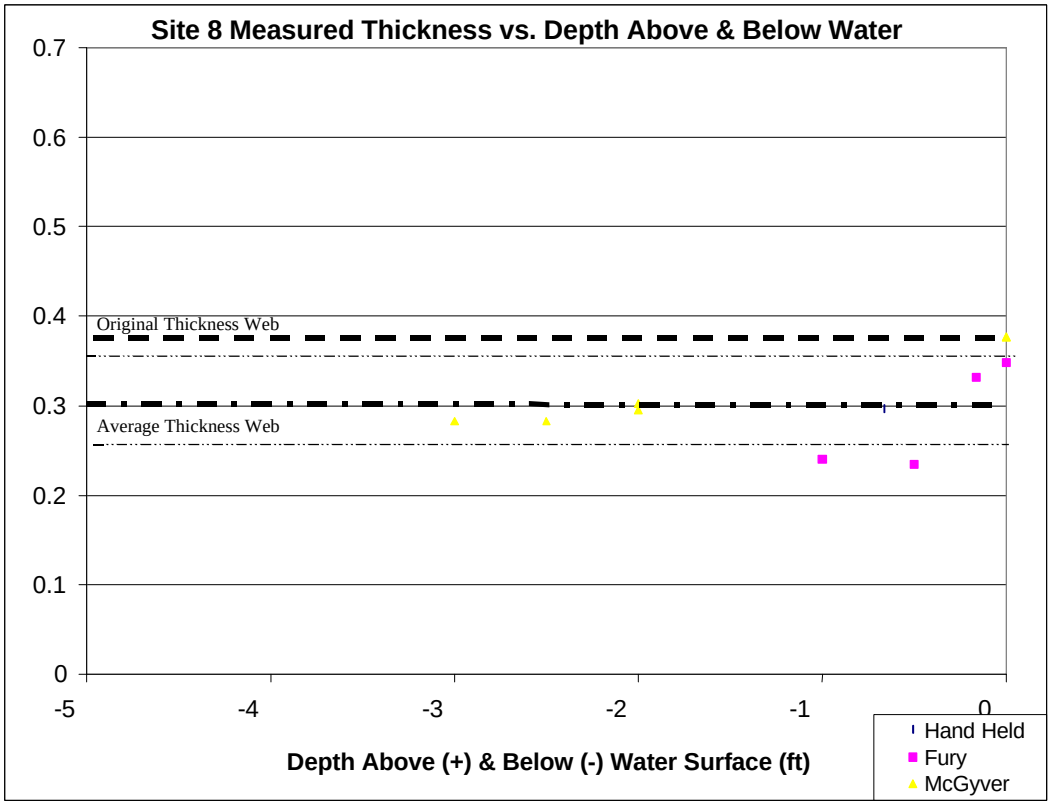

Figure 30. Site 8 thickness measurements.

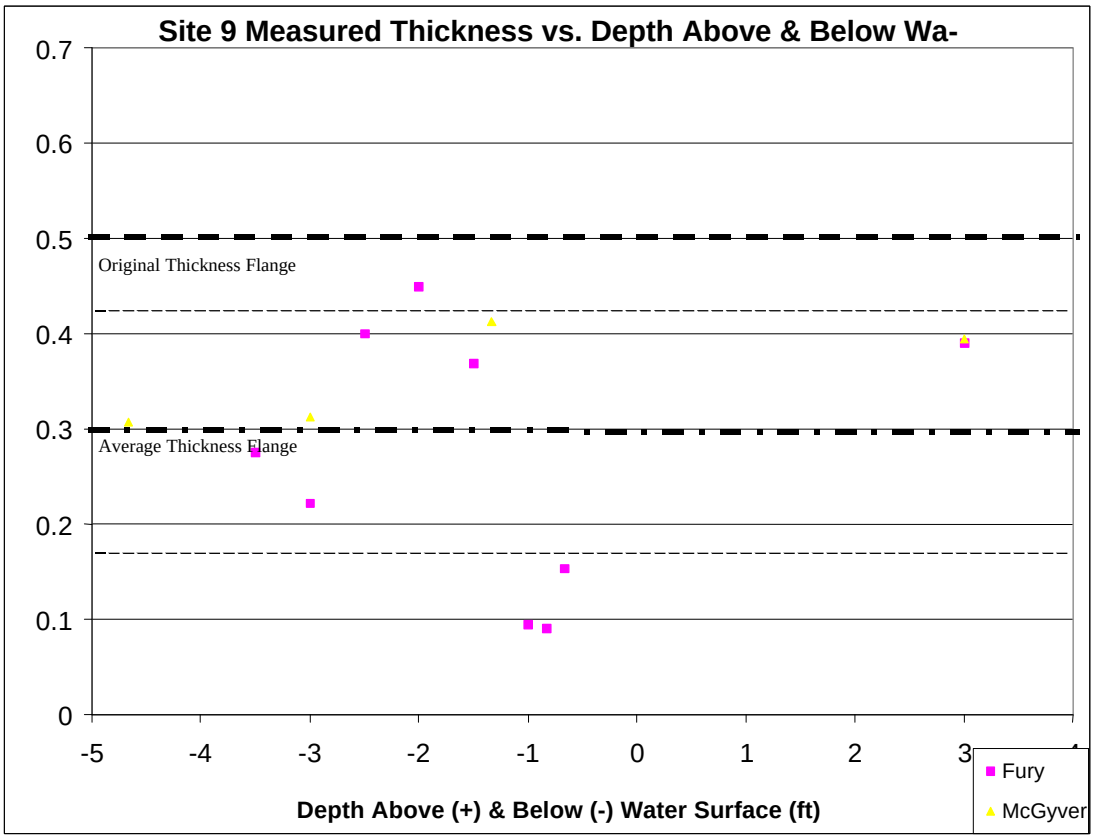

Figure 31. Site 9 thickness measurements.

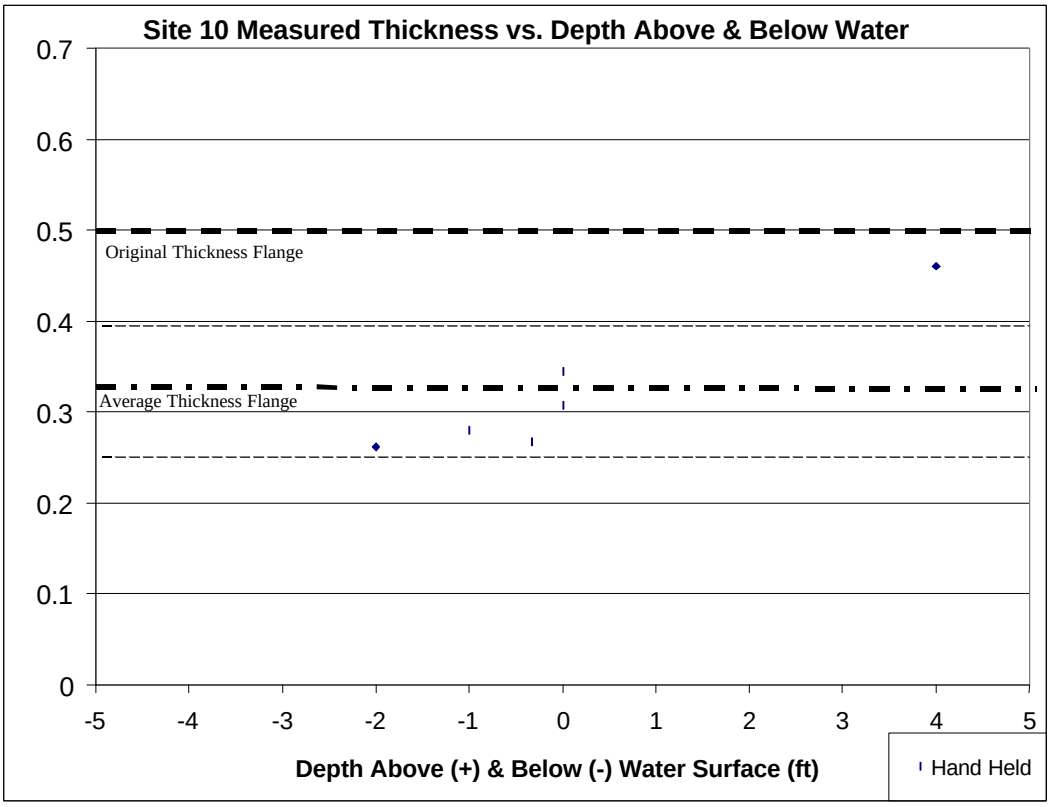

Figure 32. Site 10 thickness measurements.

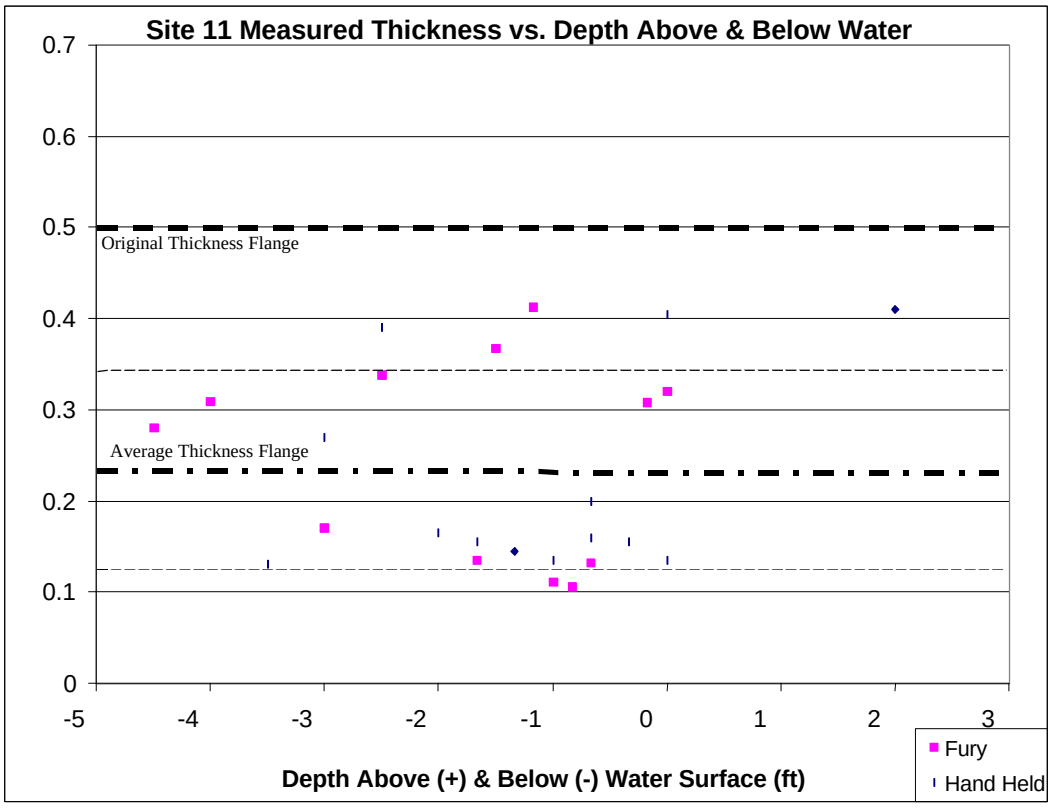

Figure 33. Site 11 thickness measurements.

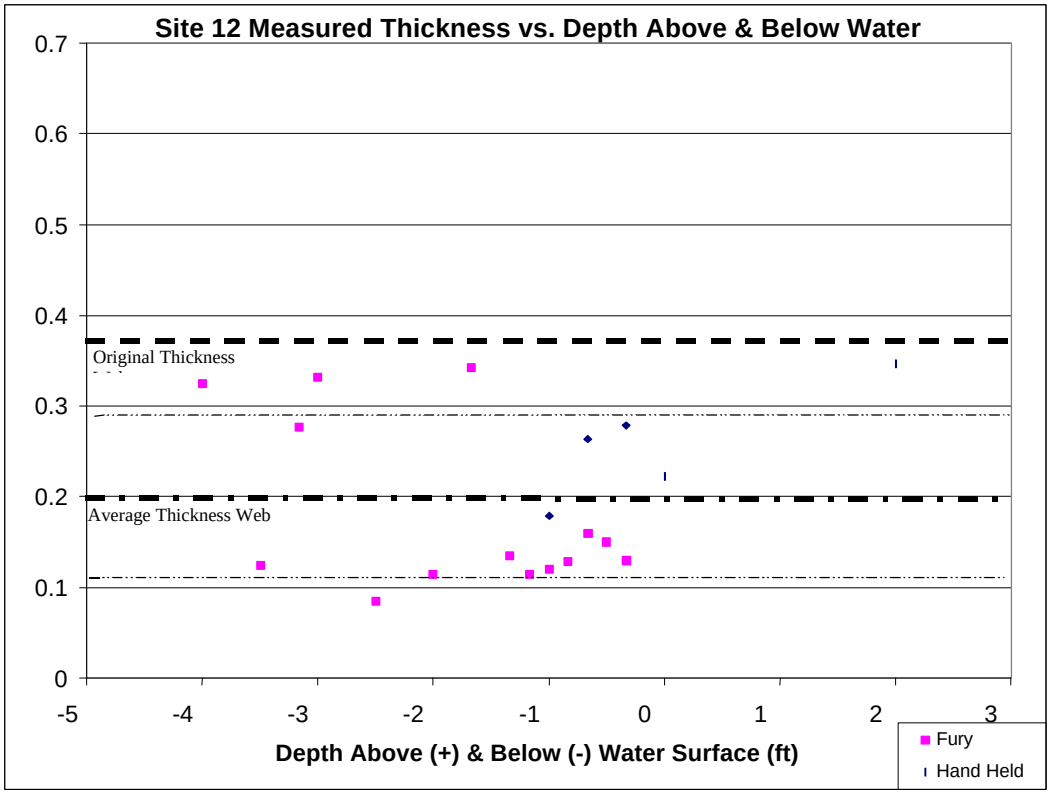

Figure 34. Site 12 thickness measurements.

Appendix A: Sites Referenced in Sheet Pile Thickness and Corrosion Rate Measurements

Note: Acoustic measurements were made by either the Panametric transducer or the transducer on the Fury robot.

Site 1

Site 1 Location: Parks1/Parks 3, City of Cleveland Parks and Recreation, next to Frank Morrison and Son; just north of marker 540 on east shore.

Type of sheet pile: cold-rolled.

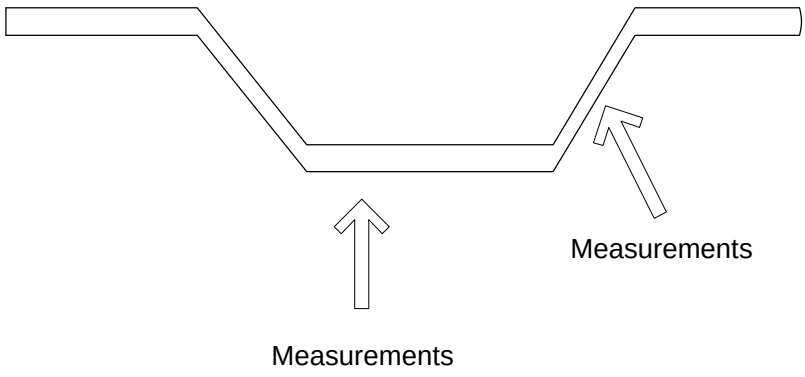

Measurements: Taken on the northeastern side approximately 40 ft upriver from water fountain. Measurements were taken on the flange and the web of the sheet pile.

Site 2

Site 2 Location: Glazer 4/City of Cleveland 32 or City of Cleveland 31, approximately 400 ft south of Site 1 between markers 540 and 548 on east shore.

Type of sheet pile: cold-rolled.

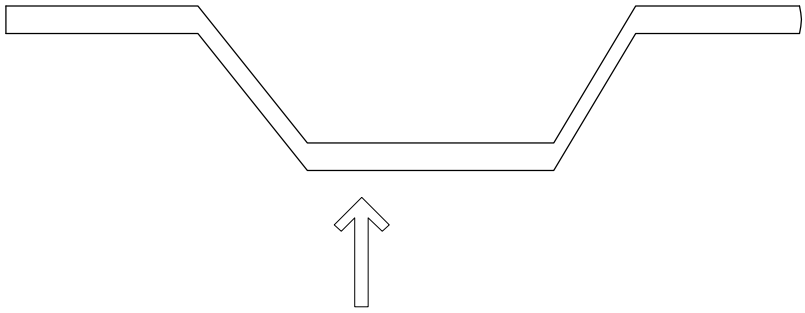

Measurements: Taken from the first full sheet pile section down from the platform on the bulkhead. All measurements were taken on the flange of the sheet pile.

Site 3

Site 3 Location: Cereal 1 / Cereal 2 or Cereal Food Processors 3, just north of marker 559 on the east shore.

Type of sheet pile: hot-rolled in front.

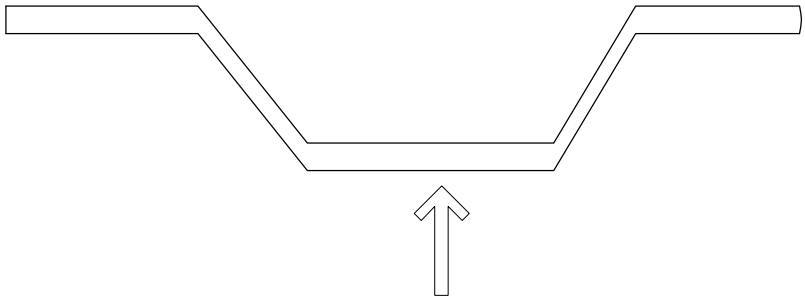

Measurements: Taken below the yellow triangle next to the 624A marker on the sheet pile, near the northwest corner of the grain loading tower. All measurements were taken on the flange of the hot-rolled sheet pile.

Site 4

Site 4 Location: Mid-Continental Coal/Coke 2, halfway between markers 640 and 650 on the east shore.

Type of sheet pile: hot-rolled.

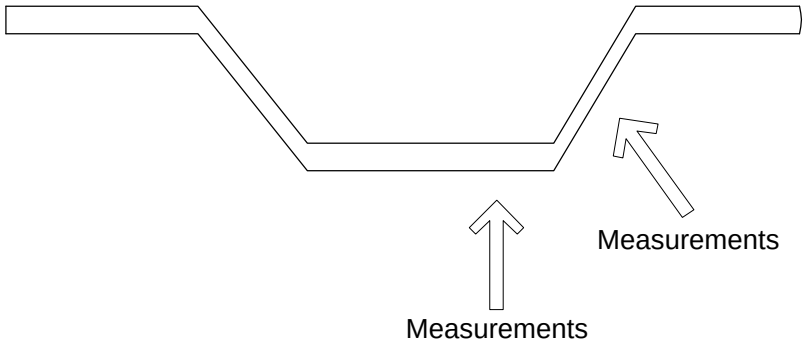

Measurements: Measurements taken close to the 650 sheet pile marker. Measurements were taken on the flange of the sheet pile by Fury and Panametrics. Panametrics measurements were also taken on the web.

Site 5

Site 5 Location: Erie RR 10/Sta Realty 2, on outcropping between markers 660 and 670, closer to 670 on west shore.

Type of sheet pile: hot-rolled.

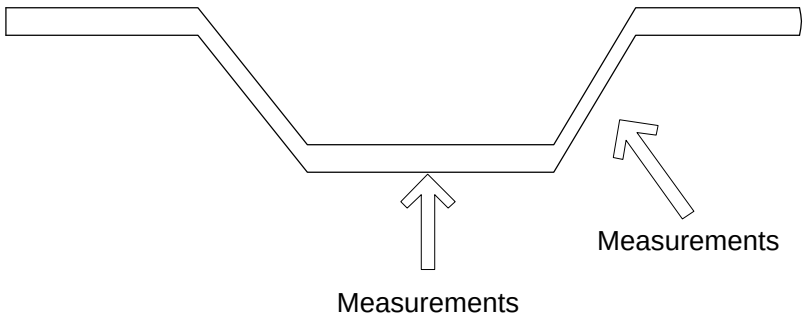

Measurements: Two measurements were taken on the web by Panametrics. All other measurements were taken on the flange by Fury and Panametrics.

Site 6

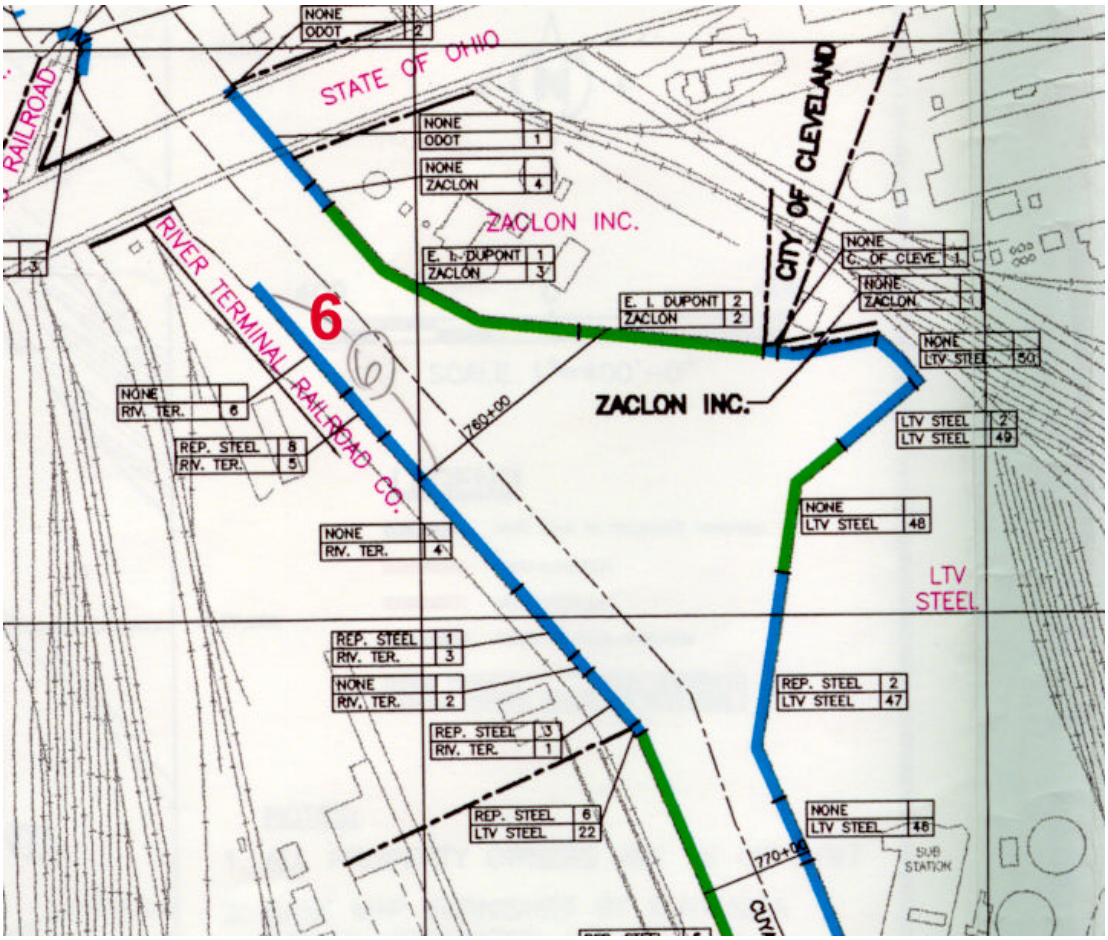

Site 6 Location: River Terminal 6, just north of marker 760 on southwest shore.

Type of sheet pile: hot-rolled.

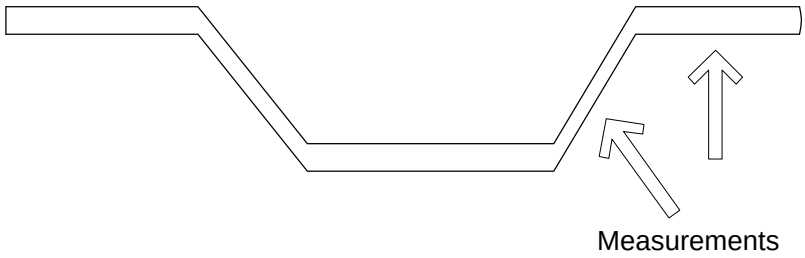

Measurements: Measurements were taken on the back flange of the sheet pile by Fury. Panametrics measurements were taken on the web.

Site 7

Site 7 Location: Carter 1, between Samsel Realty and Carter Peninsula; just south of marker 610 on the east shore.

Type of sheet pile: hot-rolled.

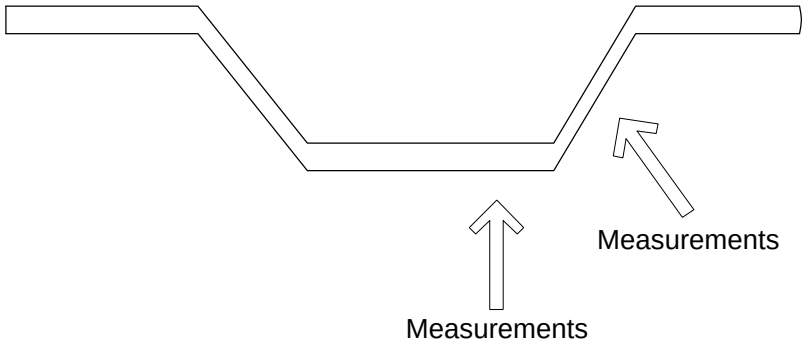

Measurements: Taken near station 610+00. Two measurements were taken on the flange of the sheet pile by Panametrics. All other measurements were taken by Fury and Panametrics on the web.

Site 8

Site 8 Location: B&O RR 1/ Tower City 1, between Tower City and F.C. Southridge Corp.; between markers 620 and 630 on the north shore.

Type of sheet pile: hot-rolled.

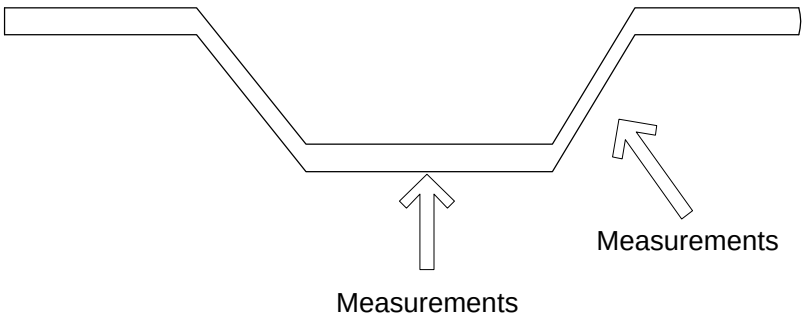

Measurements: Measurements were taken on the flange of the sheet pile by Fury and Panametrics. Panametrics measurements were also taken on the web.

Site 9

Site 9 Location: B&O RR 1/Mid-Continental 5, between markers 630 and 640, on east shore.

Type of sheet pile: hot-rolled.

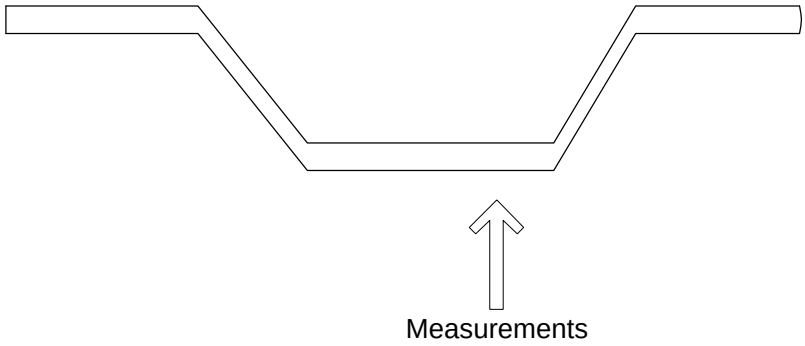

Measurements: All measurements were taken on the flange by Panametrics.

Site 10

Site 10 Location: Republic Steel 7/ LTV Steel 31, between 800 and 810 on the east shore.

Type of sheet pile: hot-rolled.

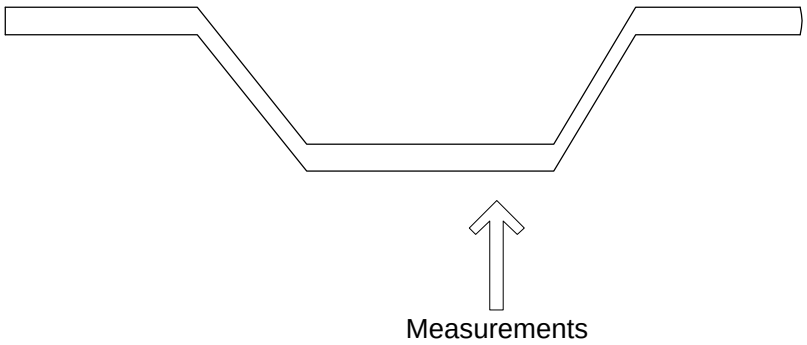

Measurements: Close to station 800+50, at front of Sun Oil terminal. All measurements were taken on the flange of the sheet pile by Fury and Panametrics.

Site 11

Site 11 Location: B&O Railroad 7 / B&O Railroad 5, slightly east of marker 700 on the north shore.

Type of sheet pile: hot-rolled.

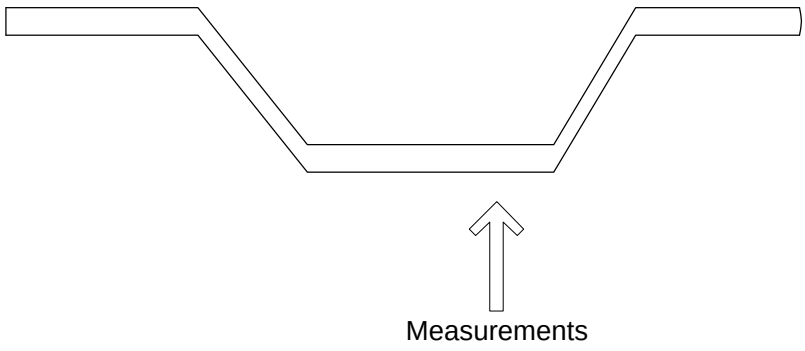

Measurements: All measurements were taken on the flange of the sheet pile by Fury and Panametrics.

Site 12

Site 12 Location: Erie RR 6 / Ontario Stone 4, between markers 320 and 310 on the south shore.

Type of sheet pile: hot-rolled.

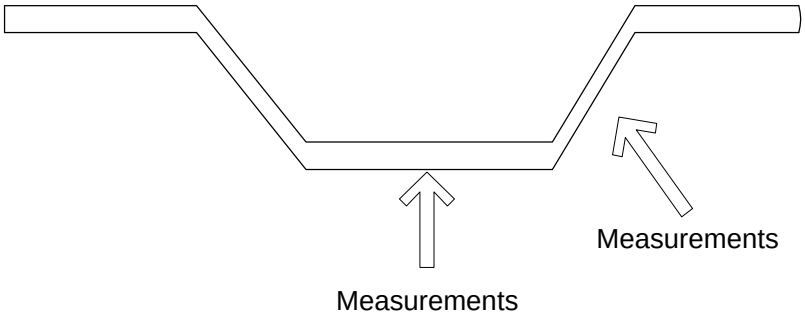

Measurements: Site near the end of the building. Measurements were taken on the web by Fury and Panametrics. One Panametrics measurement was taken on the flange.

Appendix B: Sheet Pile Thickness Measurements

Site 1 measurements were taken on 24 – 26 August 1998. The water surface was approximately 72 inches from the top of the concrete deck surface. The sheet pile at this site was cold-rolled.

Table 4. Site 1 thickness measurements.

Fury		Hand Held		Hand Held Front Face		Hand Held Short cable / side	
Height (ft)	Thickness (in)	Height (ft)	Thickness (in)	Height (ft)	Thickness (in)	Height (ft)	Thickness (in)
-1 1/2	0.438	1	0.25	3	0.5	0	0.42
-2 5/12	0.25	0	0.2	0	0.495	-1	0.48
-2 5/6	0.41	0	0.225	- 1/3	0.495	-1 1/2	0.44
-3 1/2	0.45	- 1/3	0.22	-2 1/2	0.48	-2 1/2	0.375
-3 1/2	0.462	- 2/3	0.302	-3	0.45		
-4	0.483	-1	0.28				
-4	0.48	-1	0.295				
-4 1/2	0.45	-1 1/3	0.32				
-5	0.435	-1 2/3	0.32				
-6	0.4	-2	0.25				
-6	0.4	-2	0.25				
		-3	0.26				
		-3	0.285				
		-4	0.305				
		-5	0.275	Sum T (in)	2.42	Sum T (in)	1.715
		-7 1/2	0.267	Number P	5	Number P	4
				Average T		Average	
		-7 1/2	0.215	(in)	0.484	T (in)	0.42875
		-10	0.225				
		-12	0.335			Site 1 Total	
		-13	0.26			Sum T (in)	14.132
Sum T (in)	4.658	Sum T (in)	5.339			Number P	40
						Average	
Number P	11	Number P	20			T (in)	0.3533
Average T		Average T					
(in)	0.423455	(in)	0.26695			STD =	0.0997862

Sum T stands for the sum of all thickness measurements. Number P is the number of thickness measurements, and Average T is the average thickness.

Site 2 measurements were taken on the 25 and 28 August 1998. The water surface was approximately 137 in. from the top of the piles during the first set of measurements and 133 in. from the top of the piles during the second set. All height measurements have been normalized to the first day's height data. The sheet pile at this site was cold-rolled.

Table 5. Site 2 thickness measurements.

Hand Held		Hand Held 2nd Short Cable		Fury		Fury 2nd	
Height (ft)	Thickness (in)	Height (ft)	Thickness (in)	Height (ft)	Thickness (in)	Height (ft)	Thickness (in)
4	0.375	1 2/3	0.375	4	0.323	- 1/3	0.362
0	0.37	- 1/3	0.4	0	0.341	- 1/2	0.321
- 1/3	0.377	- 2/3	0.41	-1	0.294	- 5/6	0.33
- 2/3	0.382	-1	0.395	-1 1/2	0.339	-1	0.41
-1	0.425	-1 1/3	0.415	-3	0.359	-1 1/6	0.334
-1	0.425	-1 2/3	0.4			-1 1/3	0.38
-1 1/3	0.397	-2	0.375			-1 1/2	0.375
-1 2/3	0.427	-2 1/3	0.41			-1 2/3	0.362
-2	0.455	-2 2/3	0.365			-1 5/6	0.369
-2 1/2	0.492	-3 1/3	0.42			-2	0.352
-3	0.465	-3 5/6	0.43			-2 1/6	0.362
-4	0.366					-2 1/3	0.365
-5	0.342					-2 5/6	0.36
-5	0.33					-3 1/3	0.395
-6	0.407					-3 5/6	0.342
-7	0.38					-4 1/3	0.38
-8	0.34					-4 5/6	0.4
-9	0.345					-5 1/3	0.374
-10	0.405					-5 5/6	0.388
-11	0.342					-6 1/3	0.4
						-6 5/6	0.389
						-8 1/3	0.43
						-8 5/6	0.44
						-9 1/3	0.28
						-9 5/6	0.32
Sum T (in)	7.847	Sum T (in)	4.395	Sum T (in)	1.656	Sum T (in)	9.22
Number P	20	Number P	11	Number P	5	Number P	25
Average T (in)	0.39235	Average T (in)	0.399545455	Average T (in)	0.3312	Average T (in)	0.3688
Number P	61	Sum T(in)	23.118	Ave T(in)	0.378984	STD=	0.04049

Site 3 measurements were taken on 25 August 1998. The water surface was approximately 49 in. from the top of the sheet pile, with measurements taken below the Δ624A marker. There was severe pitting at this site. The sheet pile at this site was hot-rolled.

Table 6. Site 3 thickness measurements.

Hand Held		Fury	
Height (ft)	Thickness (in)	Height (ft)	Thickness (in)
3	0.352	- 1/2	0.322
0	0.365	-1	0.21
		-3	0.152
Sum T (in)	0.717	Sum T (in)	0.684
Number P	2	Number P	3
Average T (in)	0.3585	Average T (in)	0.228
		Site 3 Total	
		Sum T (in)	1.401
		Number P	5
		Average T (in)	0.2802
		STD Web	0.09415

Sum T stands for the sum of all thickness measurements. Number P is the number of thickness measurements, and Average T is the average thickness.

Site 4 measurements were taken on 25 and 27 August 1998. The water surface was approximately 66 in. from the top of the sheet pile. The sheet pile at this site was cold-rolled.

Table 7. Site 4 thickness measurements.

Hand Held		Fury	
Height (ft)	Thickness (in)	Height (ft)	Thickness (in)
3	0.5	-1 1/6	0.4
3	0.345	-1 3/7	0.38
0	0.255	-1 1/2	0.398
- 1/3	0.415	-2	0.31
- 1/2	0.41	-2	0.15
- 2/3	0.225	-2	0.31
- 5/6	0.412	-2 1/4	0.15
-1	0.45	-2 1/4	0.25
-1	0.245	-2 3/7	0.1
-1 1/3	0.405	-2 3/7	0.38
-1 2/3	0.315	-2 5/6	0.3
-1 2/3	0.44	-3	0.32
-2	0.445	-3	0.315
-2	0.33	-3 1/2	0.24
-2 1/2	0.345	-4 1/2	0.17
-2 1/2	0.377	-4 1/2	0.318
-3	0.335	-5 1/6	0.23
		-5 5/12	0.32
		-5 1/2	0.38
		-7	0.26
		-7 2/3	0.25
Sum T (in)	6.249	Sum T (in)	5.931
Number P	17	Number P	21
Average T (in)	0.367588	Average T (in)	0.282429

Site 4 Total	
Sum T (in)	12.18
Number P	38
Average T (in)	0.320526
STD =	0.092468

Sum T stands for the sum of all thickness measurements. Number P is the number of thickness measurements, and Average T is the average thickness.

Site 5 measurements were taken on 25 and 28 August 1998. The data from the 25th consisted of only one data point due to the scale. The water surface was approximately 66 in. from the top of the sheet pile. In addition there was heavy backside scale at this site. The sheet pile at this site was hot-rolled.

Table 8. Site 5 thickness measurements.

Hand		Fury		Hand Front Face	
Height (ft)	Thickness (in)	Height (ft)	Thickness (in)	Height (ft)	Thickness (in)
2	0.526	- 1/6	0.485	3	0.397
0	0.521	- 5/6	0.126	2	0.387
- 1/3	0.228	-1	0.107		
- 2/3	0.273	-1 1/6	0.132		
-1	0.293	-1 1/3	0.162		
-1 1/3	0.223	-1 1/2	0.17		
-1 2/3	0.218	-1 2/3	0.15		
-2	0.228	-1 5/6	0.123		
-2 1/2	0.307	-2	0.192		
-3	0.223	-2 1/2	0.426		
-3 1/2	0.208	-3	0.161		
-4	0.307	-3 1/2	0.121		
		-4	0.119		
		-4 1/2	0.164		
		-5	0.189		
		-5 1/2	0.133		
		-6	0.193		
		-6 1/2	0.34		
		-7	0.178		
		-7 1/2	0.38		
		-8	0.115		
Sum T (in)	3.555	Sum T (in)	4.166	Sum T (in)	0.784
Number P	12	Number P	21	Number P	2
Average T (in)	0.29625	Average T (in)	0.198381	Average T (in)	0.392

Site 5 Tot Web	
Sum T (in)	7.721
Number P	33
Average T (in)	0.23397
STD Web	0.11898

Site 5 Tot Flange	
Sum T (in)	0.784
Number P	2
Average T (in)	0.392
STD Fl	0.007071

Sum T stands for the sum of all thickness measurements. Number P is the number of thickness measurements, and Average T is the average thickness.

Site 6 measurements were taken on 25 August 1998. The water surface was approximately 84 in. from the top of the sheet pile. The sheet pile at this site was hot-rolled.

Table 9. Site 6 thickness measurements.

Hand Short Cable Side		Hand Long Cable		Fury	
Height (ft)	Thickness (in)	Height (ft)	Thickness (in)	Height (ft)	Thickness (in)
- 1/3	0.205	0	0.21	0	0.22
- 2/3	0.215	- 1/2	0.225	- 1/2	0.225
-1	0.205	- 4/7	0.25	- 3/5	0.25
-1 1/3	0.21	-2 1/2	0.19	-2 1/6	0.21
-1 2/3	0.215	-3	0.305	-2 1/2	0.3
-1 1/3	0.335			-3	0.21
-2	0.22			-3	0.34
-2	0.284				
-6	0.357				
-7	0.34				
Sum T (in)	2.586	Sum T (in)	1.18	Sum T (in)	1.755
Number P	10	Number P	5	Number P	7
Average T (in)	0.2586	Average T (in)	0.236	Average T (in)	0.250714

Site 6 Tot	Web
Sum T (in)	5.521
Number P	22
Average T (in)	0.250955
STD Web	0.053933

Sum T stands for the sum of all thickness measurements. Number P is the number of thickness measurements, and Average T is the average thickness.

Site 7 measurements were taken on 26 August 1998. The water surface was approximately 61 in. from the top of the sheet pile. The sheet pile at this site was hot-rolled.

Table 10. Site 7 thickness measurements.

Hand		Fury		Hand Front Face	
Height (ft)	Thickness (in)	Height (ft)	Thickness (in)	Height (ft)	Thickness (in)
5	0.335	- 1/6	0.335	5	0.465
0	0.29	- 1/3	0.35		
0	0.27	- 1/2	0.3		
- 1/3	0.325	-2	0.325		
- 2/3	0.355	-2 1/2	0.285		
-1	0.35	-3	0.2		
-2	0.315	-4 1/2	0.25		
-2 1/2	0.275				
-3	0.34				
Sum T (in)	2.855	Sum T (in)	2.045	Sum T (in)	0.465
Number P	9	Number P	7	Number P	1
Average T (in)	0.317222	Average T (in)	0.292143	Average T (in)	0.465

Site 7 Tot	Web
Sum T (in)	4.9
Number P	16
Average T (in)	0.30625
STD Web	0.042642

Sum T stands for the sum of all thickness measurements. Number P is the number of thickness measurements, and Average T is the average thickness.

Site 8 measurements were taken on 25 August 1998. The water surface was approximately 65 in. from the top of the sheet pile. The sheet pile at this site was hot-rolled.

Table 11. Site 8 thickness measurements.

McGyver Side		Hand		Fury	
Height (ft)	Thickness (in)	Height (ft)	Thickness (in)	Height (ft)	Thickness (in)
0	0.377	- 2/3	0.297	0	0.348
0	0.377			- 1/6	0.332
-2	0.295			- 1/2	0.235
-2	0.302			-1	0.24
-2 1/2	0.282				
-3	0.282				
Sum T (in)	1.915	Sum T (in)	0.297	Sum T (in)	1.155
Number P	6	Number P	1	Number P	4
Average T (in)	0.319167	Average T (in)	0.297	Average T (in)	0.28875

Site 8 Total	
Sum T (in)	3.367
Number P	11
Average T (in)	0.306091
STD Web	0.048259

Sum T stands for the sum of all thickness measurements. Number P is the number of thickness measurements, and Average T is the average thickness.

Site 9 measurements were taken on 26 August 1998. The water surface was approximately 63 in. from the top of the sheet pile. The sheet pile at this site was hot-rolled.

Table 12. Site 9 thickness measurements.

McGyver w/press		Fury	
Height (ft)	Thickness (in)	Height (ft)	Thickness (in)
3	0.395	3	0.39
-1 1/3	0.412	- 2/3	0.154
-3	0.312	- 5/6	0.09
-4 2/3	0.307	-1	0.095
-5 1/3	0.335	-1 1/2	0.369
		-2	0.45
		-2 1/2	0.4
		-3	0.222
		-3 1/2	0.276
Sum T (in)	1.761	Sum T (in)	2.446
Number P	5	Number P	9
Average T (in)	0.3522	Average T (in)	0.271778

Site 9 Tot	Flange
Sum T (in)	4.207
Number P	14
Average T (in)	0.3005
STD Fl	0.118466

Sum T stands for the sum of all thickness measurements. Number P is the number of thickness measurements, and Average T is the average thickness.

Site 10 measurements were taken on 26 August 1998. The water surface was approximately 98 in. from the top of the sheet pile. The surface was uneven and there were the beginnings of pitting corrosion. The sheet pile at this site was hot-rolled.

Table 13. Site 10 thickness measurements.

Hand Held	
Height (ft)	Thickness (in)
4	0.46
0	0.345
0	0.307
- 1/3	0.267
-1	0.28
-2	0.262
Sum T (in)	1.921
Number P	6
Average T (in)	0.320167

Site 10 Tot	Flange
Sum T (in)	1.921
Number P	6
Average T (in)	0.320167
STD Fl	0.075056

Sum T stands for the sum of all thickness measurements. Number P is the number of thickness measurements, and Average T is the average thickness.

Site 11 measurements were taken on 27 August 1998. The water surface was approximately 72 in. from the top of the sheet pile. The surface was covered in a heavy coating of growth or scale and was very difficult to get clean. The sheet pile at this site was hot-rolled.

Table 14. Site 11 thickness measurements.

Fury		Hand Held	
Height (ft)	Thickness (in)	Height (ft)	Thickness (in)
0	0.321	2	0.41
- 1/6	0.308	0	0.405
- 2/3	0.132	0	0.135
- 5/6	0.106	- 1/3	0.155
-1	0.112	- 2/3	0.16
-1 1/6	0.412	- 2/3	0.2
-1 1/2	0.367	-1	0.135
-1 2/3	0.135	-1 1/3	0.145
-2 1/2	0.338	-1 2/3	0.155
-3	0.17	-2	0.165
-4	0.31	-2 1/2	0.39
-4 1/2	0.28	-3	0.27
		-3 1/2	0.13
Sum T (in)	2.991	Sum T (in)	2.855
Number P	12	Number P	13
Average T (in)	0.24925	Average T (in)	0.219615

Site 11 Tot	Flange
Sum T (in)	5.846
Number P	25
Average T (in)	0.23384
STD Fl	0.108926

Sum T stands for the sum of all thickness measurements. Number P is the number of thickness measurements, and Average T is the average thickness.

Site 12 measurements were taken on 28 August 1998. The water surface was approximately 50 in. from the top of the sheet pile. The sheet pile at this site was hot-rolled.

Table 15. Site 12 thickness measurements.

Hand Held		Fury	
Height (ft)	Thickness (in)	Height (ft)	Thickness (in)
2	0.347	- 1/3	0.129
0	0.223	- 1/2	0.15
- 1/3	0.278	- 2/3	0.16
- 2/3	0.263	- 5/6	0.128
-1	0.179	-1	0.12
		-1 1/6	0.115
		-1 1/3	0.135
		-1 2/3	0.342
		-2	0.115
		-2 1/2	0.085
		-3	0.331
		-3 1/6	0.277
		-3 1/2	0.1236
		-4	0.325
Sum T (in)	1.29	Sum T (in)	2.5356
Number P	5	Number P	14
Average T (in)	0.258	Average T (in)	0.181114

Site 12 Tot	Web
Sum T (in)	3.8256
Number P	19
Average T (in)	0.201347
STD Web	0.091268

Sum T stands for the sum of all thickness measurements. Number P is the number of thickness measurements, and Average T is the average thickness.

Appendix C: Sheet Pile Corrosion Rate Measurements

Definition of Current

A current value of (-)1.2 mA can mean different things to workers in different areas of electrochemistry. To an analytical electrochemist, it represents 1.2 mA of anodic current. To a corrosion scientist, it represents 1.2 mA of cathodic current. In the techniques used by the test equipment for this project, the corrosion convention for current was followed. Positive currents are anodic, resulting in an oxidation at the metal specimen under test.

Potential Values and Conventions Used in this Analysis

In this study, the equilibrium potential assumed by the metal in the absence of electrical connections to the metal is called the open circuit potential (E_{oc}). The term corrosion potential (E_{corr}) was reserved for the potential at which no current flows, as determined by a numerical fit of current versus potential data. In an ideal case, the values for E_{oc} and E_{corr} will be identical. One reason the two voltages may differ is changes in the electrode surface during the scan. In this study, all potentials are specified or reported as the potential of the working electrode with respect to either the reference electrode or the open circuit potential. The former is always labeled as "vs E_{ref}" and the latter is labeled as "vs E_{oc}". The equations used to convert from one form of potential to the other are:

$$E \text{ vs } E_{oc} = (E \text{ vs } E_{ref}) - E_{oc} \quad \textbf{[Eq C1]}$$

$$E \text{ vs. } E_{ref} = (E \text{ vs } E_{oc}) + E_{oc} \quad \textbf{[Eq C2]}$$

Regardless of whether potentials are versus E_{ref} or versus E_{oc}, one sign convention is used. The more positive a potential, the more anodic it is. More anodic potentials tend to accelerate oxidation of a metal specimen.

Nearly all metal corrosion occurs via electrochemical reactions at the interface between the metal and an electrolyte solution. A thin film of moisture on a metal surface forms the electrolyte for atmospheric corrosion. Wet concrete is the electrolyte for reinforcing rod corrosion in bridges.

Corrosion normally occurs at a rate determined by equilibrium between opposing electrochemical reactions. The first is the anodic reaction, in which a metal is oxidized, releasing electrons into the metal. The other is the cathodic reaction, in which a solution species (often o_2 or H^+) is reduced, removing electrons from the metal. When these two reactions are in equilibrium, the flow of electrons from each reaction is balanced, and no net electron flow (electronic current) occurs. The two reactions can take place on one metal or on two dissimilar metals (or metal sites) that are electrically connected.

Figure 35 diagrams this process. The vertical axis is potential and the horizontal axis is the logarithm of absolute current. The theoretical currents for the anodic and cathodic reactions are shown as straight lines. The curved line is the sum of the anodic and cathodic currents. It is the current that is measured when a sweeping scan of the potential of the metal is made. The sharp point in the curve results from the use of a logarithmic axis. It is actually the point where the current gets very small prior to changing sign.

The potential of the metal is the means by which the anodic and cathodic reactions are kept in balance (Figure 35).

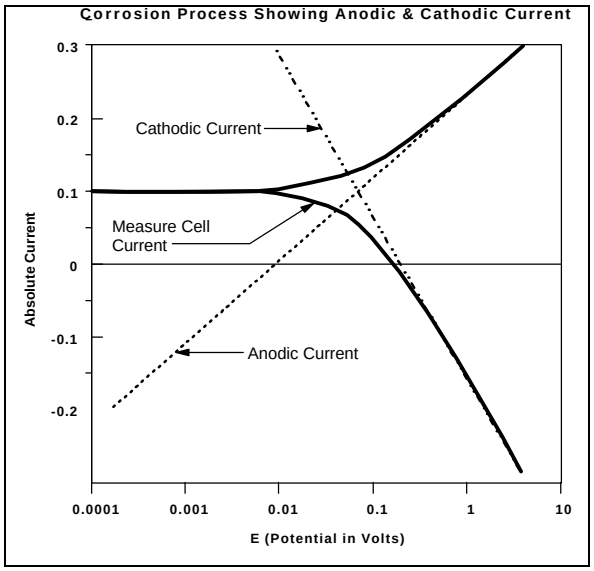

Figure 35: Corrosion process showing anodic and cathodic current. It should be noted that the current from each half reaction depends on the electrochemical potential of the metal.

Suppose the anodic reaction releases too many electrons into the metal. Excess electrons shift the potential of the metal more negative, which slows the anodic reaction and speeds up the cathodic reaction. This counteracts the initial perturbation of the system.

In the system used in this study, the equilibrium potential assumed by the metal in the absence of electrical connections to the metal is called the open circuit potential (E_{oc}).

The value of either the anodic or cathodic current at E_{oc} is called the corrosion current, I_{corr}. If we could measure I_{corr}, we could use it to calculate the corrosion rate of the metal. Unfortunately I_{corr} cannot be measured directly. However, it can be estimated using electrochemical techniques. In any real system, I_{corr} and corrosion rate are a function of many system variables including type of metal, solution composition, temperature, solution movement, metal history, and many others.

The above description of the corrosion process does not say anything about the state of the metal surface. In practice, many metals form an oxide layer on their surface as they corrode. If the oxide layer inhibits further corrosion, the metal is said to *passivate*. In some cases, local areas of the passive film break down, allowing significant metal corrosion to occur in a small area. This phenomenon is called *pitting corrosion*, or simply *pitting*.

Electrochemical Testing Techniques

Because corrosion occurs via electrochemical reactions, electrochemical techniques are ideal for the study of the corrosion processes. In electrochemical studies, a metal sample a few cm^2 in surface area is used to model the metal in a corroding system. The metal sample is immersed in a solution typical of the metal's environment in the system being studied. Additional electrodes are immersed in the solution, and all the electrodes are connected to a device called a potentiostat. A potentiostat allows the users to change the potential of the metal sample in a controlled manner.

With the exception of open circuit potential vs time and galvanic corrosion techniques, all the standard electrochemical analysis techniques utilized in this study use a potentiostat to perturb the equilibrium corrosion process. When the potential of a metal sample in solution is forced away from E_{oc}, it is referred to as *polarizing the sample*. The response (current or voltage) of the metal sample is measured as it is polarized. The response is used to develop a model of the sam-

ple's corrosion behavior. Both controlled potential (potentiostatic) and controlled current (galvanostatic) polarization is useful. When the polarization is done potentiostatically, current is measured, and when it is done galvanostatically, potential is measured. This discussion will concentrate on controlled potential methods, which see more common use.

Suppose we use the potentiostat to force the potential of a metal anodic (toward positive potentials) from EOC. In Figure 35, we are moving toward the top of the graph. This will increase the rate of the anodic reaction and decrease the rate of the cathodic reaction. Since the anodic and cathodic reactions are no longer balanced, a net current will flow from the electronic circuit into the metal sample. The sign of this current is positive by convention. The potentiostat accurately measures the current. If we take the potential far enough from E_{oc}, the current from the cathodic reaction will be negligible, and the measured current will be a measure of the anodic reaction alone. In Figure 35, notice that the curves for the cell current and the anodic current lie on top of each other at positive potentials. Conversely, at strongly negative potentials, the cathodic current dominates the cell current.

In some cases, as we vary the potential, we will first passivate the metal, then cause pitting corrosion. Analysis of a curve plotting the measured current versus time or potential may allow us to determine I_{corr} at E_{corr}, the tendency for passivation to occur, and the potential range over which pitting will occur.

The polarization resistance tests run in this study utilized Gamry CMS 100 Electrochemical corrosion testing software and hardware installed in a Gateway P5-133 computer operating under Windows 95. Each polarization resistance scan run during the field testing phase required the following operations:

1. Select test site and transport test equipment to site.

2. Placement of the counter electrode (CE) and reference electrode (RE) with current containment chamber on the water-side sheet pile surface at the desired test depth and orientation (Figure 37).

3. Connect wiring to/from the working electrode (*WE* = in this case the steel sheet pile), counter electrode (*CE* = ¼" x 4" ceramic-coated titanium rod element) and reference electrode (*RE* = MC Miller Saturated Cu-$CuSO_4$ Reference Electrode) to the corresponding terminals on the Gamry Circuit Boards installed in the computer.

4. Start the "Gamry CMS100 Software" program.

5. The “Experiments” window created by the CMS100 provides a number of potentiostatic and potentiodynamic test alternatives. In this study, the " polarization Resistance Experiment" program was selected as the primary test module.

6. The program creates a “Setup” dialog box that becomes the active window and accepts changes in the experimental parameters.

7. The script then obtains the use of the potentiostat specified during Setup and opens a data file using the tester's entered Output name. In this study, all Tafel experiments were labeled “coetaf#xx.dta” while all polarization resistance (commonly called linear polarization) experiments were labeled either “coepr#xx.dta” or “coelp#xx.dta.

8. The file header information is written to the data file. This header information includes:

   a. tags identifying possible analyses
   b. the current time and date
   c. a list of the setup parameters. This information is written to the file prior to data acquisition.

   In all polarization resistance tests, the following test options were used:

   Total Potential Band to be tested – (-)20 mV to (+)20 mV from “E_{corr}”

   - potential test steps of 0.2 mV
   - potential test time of 1 second per step
   - test area of 180 cm^2
   - steel sheet pile faradaic consumption rate of 6 gm/cm^3
   - 15 second time conditioning only of test surface with NO applied current or voltage.
   - initial test setup stabilization period of 120 seconds or achievement of “E_{corr}” stability, as defined by a change of less than 0.1 mV/second for 5 consecutive readings, whichever occurs first.
   - Inputting of any relevant test notes, such as test site location, sheet pile surface being tested, depth of probe below existing water level, etc.

9. The program can first condition the electrode by applying a fixed potential for a defined time period. It can establish a known surface state on the corrosion specimen. A plot of current versus time is displayed during this conditioning. For the *in situ* corrosion testing on this project, this procedure was set at 0 volts and thus was not used as it would distort the results.

10. The E_{oc} of the sheet pile surface directly under the probe containment chamber is measured.

    a. If an initial delay is turned on in the setup, this step lasts for the time specified as the initial delay time, or until the E_{corr} potential stabilizes. During this study, the delay maximum time was set to either 180 seconds or a stabilized potential was achieved as defined by three successive readings being within +/- 0.5 mV of each other.
    b. A real-time plot of the measured sheet pile potential versus time is always displayed on the computer's display. The last potential measured after the initial delay criterion is met is recorded as E_{oc}.

11. The Polarization Resistance scan is then initiated. The potential of the sample is swept from the Initial E (E_{oc}) to the Final E. Current readings at the above-specified 1 second time intervals are taken during the sweep.

    a. The sweep is actually a staircase ramp. The sample is potentiostatic at the E_{oc}, a delay of one sample period occurs, and a reading of the current is taken.
    b. The potential is then stepped by the mV value specified (0.2 mV in this study), a delay of one sample period (1 second in this study) occurs, and the next current reading is taken.
    c. Stepping the potential, delaying and acquiring data points continues until the potential equals the final E. At each point the current range is automatically switched to the optimal range for the measured cell current.
    d. IR-drop error compensation was used in each scan, correcting each potential for the measured IR drop of the preceding point.
    e. A plot of log I vs E is displayed during the scan.

12. The data are written to the output file and the script cleans up and halts.

13. When the scan is over the cell is turned off, after which the next location can be tested.

14. The data are then analyzed by a separate program module which runs as a subroutine under Microsoft Excel. The program automatically evaluates the measured data in accordance with Stern-Geary equation (discussed in more detail in Section V of this report), and the graphs and data including corrosion rate (CorrRate) are displayed and printed out in the form shown in Figure 35.

Figure 36. Coal storage at Site 4, the Mid-Continental Coke and Coal property.

Figure 37. Polarization resistance testing device.

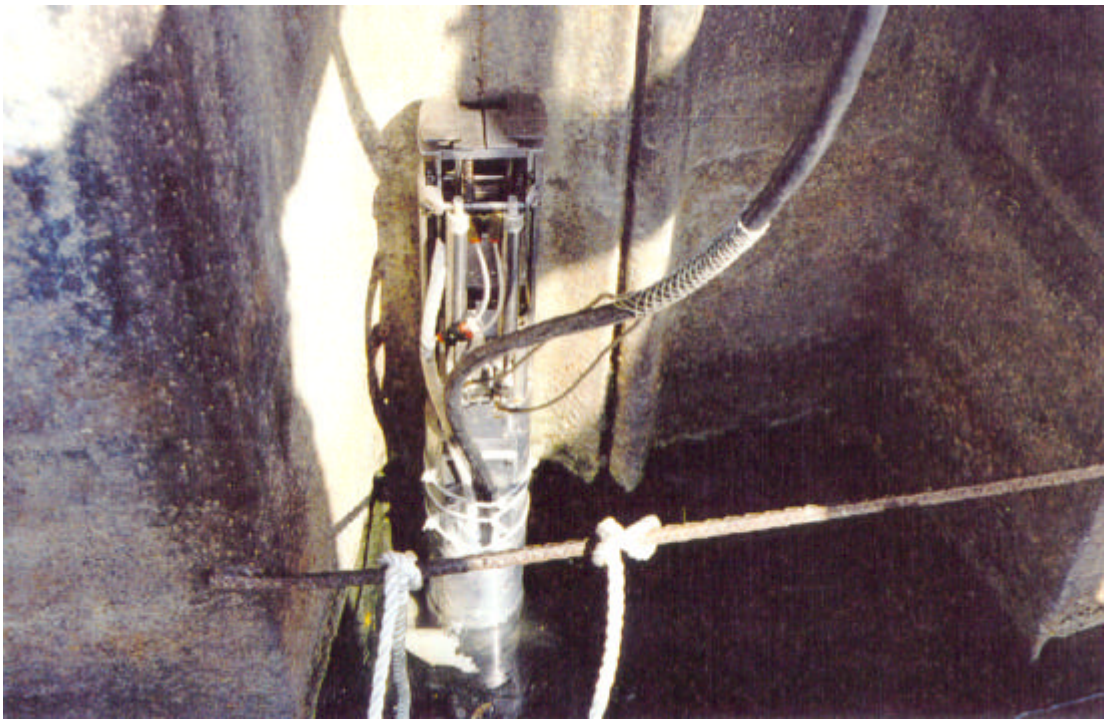

Figure 38. Fury robot entering the water on the back flange of the sheet pile.

Figure 39. Fury nearly submerged, taking measurements on the front flange of sheet pile.

Appendix D: Resistivity and Water Chemistry Data

Cuyahoga River Basin
Water Quality Data for 1996 Survey
Rewrite

Station	River Mile	Date	Time	Comments	TEMP	pH	D.O.	COND.	Hardness as CACO3	NO2-NO3	NH3-N	TKN	TDS
Cuy R@ W3rd St.	3.26	04-Sep-96	1118		27.5	7.3	5.2	1190	266	8.56	0.52	1.5	702
Cuy R@ W3rd St.	3.26	10-Jul-96	1216		26.9	7.65	4.0	1011	276	7.56	0.62	1.7	728
Cuy R@ W3rd St.	3.26	20-Jun-96	1015	Ore Boat 20 Mins. Ago	23.3	7.6	8.7	650	177	2.66	0.37	1.1	392
Cuy R@ W3rd St.	3.26	29-Aug-96	1105		27.0	7.6	4.9	1070	257	7.64	0.40	0.5	644
Cuy R@ W3rd St.	3.26	20-Jul-96	1153		26.5	7.6	3.5	1150	250	6.83	0.61	1.7	684
Cuy R@ dst Columbus Ave.	1.46	04-Sep-96	1149		27.0	7.3	3.6	1175	269	7.54	0.53	1.4	690
Cuy R@ dst Columbus Ave.	1.46	04-Sep-96	1149		27.0	7.3	3.6	1175	269	7.35	0.55	1.5	694
Cuy R@ dst Columbus Ave.	1.46	10-Jul-96	1346		26.3	7.48	4.1	1017	274	7.31	0.71	1.7	710
Cuy R@ dst Columbus Ave.	1.46	20-Jun-96	0945	Freighter Two Hours Ago	24.0	7.54	3.75	640	173	2.40	0.43	1.3	358
Cuy R@ dst Columbus Ave.	1.46	29-Aug-96	1129		27.0	7.5	2.7	1010	246	6.47	0.51	0.5	608
Cuy R@ dst Columbus Ave.	1.46	29-Aug-96	1129	CD Verified 10-1-96						6.53	0.54	0.6	610
Cuy R@ dst Columbus Ave.	1.46	30-Jul-96	1247	After Rain Started	25.0	7.4	4.1	1000	224	5.75	0.78	1.7	610
Cuy R@ dst Columbus Ave.	1.46	30-Jul-96	1247	After Rain Started	25.0	7.4	4.1	1000	222	5.65	0.75	1.6	608